Lateral Hypothalamic GABAergic neurons encode and potentiate sucrose's palatability

Aketzali Garcia, Alam Coss, Jorge Luis-Islas, Liliana Puron-Sierra, Monica Luna, Miguel Villavicencio, Ranier Gutierrez*

Laboratory of Neurobiology of Appetite; Department of Pharmacology, CINVESTAV, 07360. Mexico City, Mexico.

*** Correspondence:**
Ranier Gutierrez
ranier@cinvestav.mx
ORCID: https://orcid.org/0000-0002-9688-0289

Keywords: LHA^{Vgat+} neurons, feeding circuits, palatability, sucrose

This PDF file includes:

Number of pages: 56

Number of figures: 12

Abstract

Sucrose is attractive to most species in the animal kingdom, not only because it induces a sweet taste sensation, but also for its positive palatability or likability. Although palatability is such an important sensory attribute, it is currently unknown which cell-types encode and modulate sucrose's palatability. Studies in mice have shown that GABAergic LHA^{Vgat+} neurons evoke voracious eating; however, it is not known whether these neurons would be driving consumption by increasing palatability. Using optrode recordings, we measured sucrose's palatability while VGAT-ChR2 transgenic mice performed a brief access sucrose test. We found a subpopulation of LHA^{Vgat+} neurons that their activity correlated with the increase in licking responses evoked by sucrose concentrations. Optogenetic gain of function experiments where mice were able to choose among available water, 3%, or 18% sucrose solution, uncovered that opto-stimulation of LHA^{Vgat+} neurons consistently promoted higher intake of the most palatable stimuli (18% sucrose). In contrast, if they self-stimulated near the less palatable stimulus, some VGAT-ChR2 mice preferred water over 18% sucrose. Unexpectedly, activation of LHA^{Vgat+} neurons increased quinine intake but only during water deprivation, since in sated animals, they failed to promote quinine intake or to tolerate an aversive stimulus. Conversely, these neurons promoted overconsumption of sucrose when it was the nearest stimuli. We conclude that a subpopulation of LHA^{Vgat+} neurons increases tastant's intake by potentiating its palatability.

Introduction

The Lateral Hypothalamic Area (LHA) has been regarded as the "feeding center" since its lesion results in hypophagia and subsequent death [1,2]. It is part of a neural circuit related to feeding and reward [3,4] as rats are willing to press a lever to deliver electrical intra-cranial self-stimulation (ICSs), and if food is available, it also promotes feeding [3,5–7]. Moreover, if a sweet tastant is available, the rate of electrical ICSs is further increased, whereas bitter compounds decreased ICSs rates [8,9], suggesting an interaction between ICSs and taste palatability. In this regard, and because of its connections with different cortical and subcortical gustatory regions [10–13], the LHA is anatomically located to processes and broadcast taste palatability information [14,15]. Pioneering electrophysiological studies have recorded gustatory-evoked responses in the LHA [16,17]. One recent study uncovered two functional populations of LHA neurons: one that was activated by palatable tastants, e.g., sucrose, and the other by aversive tastants, like quinine [18]. However, the genetic identity of the LHA cell-type(s) involved in processing palatability-related information remains elusive, and to unveil their identity is a goal of this study.

The LHA is currently viewed as a hub of various cell-types [19] grossly divided into two larger populations related to feeding: the glutamatergic ($LHA^{Vglut2+}$) and GABAergic neurons (LHA^{Vgat+}) [20]. Activation of $LHA^{Vglut2+}$ neurons leads to reduced food intake and is aversive [21]. In contrast, stimulation of LHA^{Vgat+} neurons is rewarding and produces voracious eating of both foods with nutritional value [22,23] and those without calories or even gnawing behavior towards an irrelevant biological stimulus [23]. Moreover, LHA^{Vgat+} neurons enhance the salience of the nearest stimuli and induce reward via stimulation of their projections to the ventral tegmental area (VTA) [24]. In addition, the evoked feeding is mediated by modulation of terminals reaching a region adjacent to the locus coeruleus [25]. On the contrary, inhibition of GABAergic LHA^{Vgat+} cell somas is aversive and stops

72 feeding [22,23]. However, the role of LHA^{Vgat+} neurons in processing sucrose's palatability remains to
73 be determined.

74

75 This study identified a new role of LHA^{Vgat+} neurons in encoding and enhancing sucrose's palatability.
76 We found that a subpopulation of LHA GABAergic neurons increases the consumption of the most
77 palatable and proximal tastant. They accomplish this by potentiating the palatability of nearby
78 gustatory stimuli. For aversive stimuli, the effect of these neurons is different. In a single bottle test,
79 we found that water deprivation increased the tolerance for bitter compounds and gated a window of
80 opportunity within which the activation of GABAergic neurons is sufficient to reassign the negative
81 hedonic value of quinine temporarily and promotes its intake. Nevertheless, in a three-option
82 preference test, these neurons failed to develop a preference to quinine when sucrose was available.
83 Moreover, optogenetic activation of LHA^{Vgat+} neurons evoked many hallmark behaviors resembling
84 those seen in LHA electrical stimulation. In this regard, and consistent with their positive role in
85 palatability, our results could explain why electrical ICSs are further facilitated by the presence of
86 sweet solutions [8,9]. We also found that LHA^{Vgat+} neurons are the common neural substrate for both
87 reward and feeding since after repeated self-stimulation, the more the VGAT-ChR2 mice opto-self-
88 stimulated, the stronger the laser-induced licking they exhibited. We conclude that a subpopulation of
89 GABAergic LHA^{Vgat+} neurons combines stimulus-proximity and palatability-related information to
90 enhance nearby energy-rich foods' palatability.

91

92

93

Materials and methods

Animal subjects

We used 36 VGAT-ChR2 mice from both sexes and 8-16 weeks old (number ID 014548; Jackson Laboratory, Sacramento, CA, USA). 21 wildtype (WT) littermates were used as a control, from both sexes. Mice were individually housed in laboratory home cages and maintained in a temperature-controlled (22 ± 1° C) room with 12:12 h light-dark cycle, and unless otherwise mentioned, Chow food (PicoLab Rodent Diet 20, MO, USA) and water was available *ad libitum*. For experiments with water restriction, after behavioral testing, mice were allowed to drink water for 1 h daily. All procedures were performed with the approval of the CINVESTAV Animal Care and Use Committee. Experiments were conducted at the same time of the day from 11:00 AM to 2:00 PM.

Surgical procedures

All mice were anesthetized with ketamine (100 mg/kg, i.p.) and xylazine (8 mg/kg, i.p.), and placed into a stereotaxic apparatus (Stoelting, IL, USA). Lidocaine (0.05 mL) was applied subcutaneously under the skin's head as an analgesic, and ophthalmic ointment (hydrocortisone, neomycin, and polymyxin-B) was used periodically to maintain eye lubrication. The antibiotic enrofloxacin (0.4 mL/kg) was injected for 3 days as a post-surgery recovery.

For experiments with opto-stimulation of LHA^{Vgat+} cell somas, a single multimode optical fiber 200 µm core diameter with a 0.39 NA (FT200UMT; Thorlabs, NJ, USA) was implanted unilaterally targeting the LHA using the following coordinates: AP: -1.25 mm, ML: ± 1 mm, DV: -4.9 mm, from bregma. For electrophysiology recordings, a custom-made optrode was unilaterally implanted

116 counterbalanced for both hemispheres (AP: -1.25 mm, ML: ± 1 mm, from bregma; DV: -5.2 mm
117 ventral to dura). The optrode comprises an array of 16 tungsten wires formvar coated (35 µm diameter)
118 surrounding and protruding 1 mm the single multimode optical fiber tip. No significant differences
119 were found between hemispheres, so data were pooled together (data not shown). To allow for
120 recovery, all experiments began seven days after surgery.

121

122 *Histology and Immunofluorescence*

123 To verify optrode and fiber optic location, at the end of the experiments, mice were sacrificed by an
124 overdose of pentobarbital (150 mg/kg) and perfused with PBS, followed by 4% paraformaldehyde.
125 Brains were fixed overnight in 4% paraformaldehyde and gradually replaced in a gradient of
126 concentrations until reaching 30% sucrose. For histology, brain slides (40 µm) were cut with a cryostat
127 (Thermo Scientific HM525 NX) and images were taken with a Nikon eclipse e200 microscope and a
128 Progress Gryphax microscope camera, using a 10x objective.

129

130 Free-floating brain slides (40 µm) were blocked with 1% BSA, 0.2% Triton in PBS for 30 min. Then,
131 they were washed with 0.2% Triton in PBS three times every 10 min, followed by the incubation with
132 the primary antibodies: mouse anti-GAD 67 primary antibody (Millipore, Mab5406, 1:1000 dilution)
133 and rabbit anti-GFP primary antibody (Invitrogen, A11122, 1:1000 dilution). Incubation took place
134 overnight at 4°C. The next day, brain slides were washed with 0.2% Triton in PBS three times every
135 10 min, then incubated with the secondary antibodies Alexa 647 goat anti-mouse (Invitrogen, A21235,
136 1:500 dilution) and Alexa 488 donkey anti-rabbit (Invitrogen, A21206, 1:500 dilution) during 90 min
137 at room temperature. Afterward, we applied DAPI to stain the nuclei. Brain slides were put on slides

138 with a mounting medium for fluorescence (Vectashield), and images were taken with a Leica confocal
139 microscope using a 63x objective.

140

141 *Gustatory stimuli*

142 Sucrose reagent-grade chemical quality (Sigma-Aldrich, Mexico City, Mexico) was used in the
143 following concentrations: no sucrose, 3, 10, and 18 wt%. Quinine hydrochloride dihydrate (QHCl)
144 reagent-grade was used at 0.004 wt% (Sigma-Aldrich, Mexico City, Mexico). Artificial Saliva
145 contained (mM): 4 NaCl, 10 KCl, 6 $NaHCO_3$, 6 $KHCO_3$, 0.5 $CaCl_2$, 0.5 $MgCl_2$, 0.24 K_2HPO_4, 0.24
146 KH_2PO_4 [26]. We added 0.05 mM HCl to adjust to pH 7. The solutions were dissolved in distilled
147 water, maintained under refrigeration, and used at room temperature. We also used 20 mg chocolate
148 pellets (Bio-Serv, NJ, USA), Chow food (PicoLab Rodent Diet 20, MO, USA), a high-fat diet with
149 45% kcal% fat (Research Diets, NJ, USA), granulated sugar cube, and cork.

150

151 *Optogenetic stimulation*

152 A 473 nm laser intensity was modulated by a DPSS system (OEM laser, UT, USA). Laser pulses were
153 synchronized with behavioral experiments with Med Associates Inc. software and TTL signal
154 generator (Med Associates Inc., VT, USA). The optical power at the patch cord was 15 mW, and it
155 was measured with an optical power meter (PM20A, Thorlabs, NJ, USA). This delivers between 10 to
156 12.6 mW at the tip of the fiber optic, depending on each fiber's efficiency. To explore the best
157 stimulation parameters for LHA GABAergic neurons, the laser was turned "on" at different frequencies
158 2.5, 5, 10, 20, and 50 Hz semi-randomly, with a 10 ms pulse width. For the other experiments, the laser
159 was fixed at 50 Hz. The laser was 2 s on and 4 s off, with 10 ms pulse width and a duty cycle of 50%.

Behavioral Assays

Pre-stimulation task

Mice were placed in an operant conditioning chamber with a central port, a door blocked the access to the sipper during the first 15 min. In this pre-stimulation period, each mouse was opto-stimulated with all pre-stimulation parameters following a Latin square design (described in Table 1). Then, the door was opened and a 10% sucrose solution was available during the next 15 min. During the pre-stimulation period, the laser was turned on for 2 s and off for 4 s.

Table 1. Pre-stimulation protocol schemes:

Laser on	Sucrose access
0 min	15 min
5 min	15 min
10 min	15 min
15 min	15 min

Open loop stimulation task

Mice were opto-stimulated by alternating 5 min off and 5 min on blocks across the session [24]. During opto-stimulated blocks, the laser was turned "on" regardless of the mice's behavior and spatial position in the chamber. The front panel of an operant conditioning chamber (Med Associates Inc, VT, USA) was equipped with one or three ports, each with a sipper where individual licks were registered by a contact lickometer (Med Associates Inc, VT, USA). To determine the best stimulation parameters to induced feeding behavior, a group of naïve mice was tested with one single port, and in each session a different opto-stimulation frequency (0, 2.5, 5, 10, 20, and 50 Hz) was delivered daily. Mice had free access to a single sucrose 10% solution in the central port.

178 To determine whether opto-stimulation of LHA GABAergic neurons bias the intake towards the most
179 palatable stimuli available. A different group of mice was tested in an open loop stimulation task, in a
180 box equipped with three ports, where mice had free access to water (central sipper), a 3% sucrose
181 solution (left sipper), and 18% sucrose solution (right sipper). Lateral sippers were counterbalanced
182 across animals. This task comprised of 4 baseline days (with no opto-stimulation, data not shown) and
183 11 test days.

184

185 For the open loop stimulation sessions, with three ports, we video tracked the mouse's distance and
186 head angle relative to each of the three sippers. The sippers' position and three anatomical animal's
187 points, the nose, the neck, and the tail's base, were extracted using the DeepLabCut Python package
188 [27,28]. We define the mouse position as the coordinates (x and y) for the nose, whereas the head
189 direction was a 2D vector going from the neck to the nose. For each video frame, the relative distance
190 to each sipper was calculated (in pixels), and the relative angle between the head direction and position
191 of each sipper (in degrees). An angle of 0º means the mouse is looking at the sipper, and 180º means
192 facing in the opposite direction. For distance measuring, 100 pixels correspond to approximately 6 cm.
193 The mouse position and direction were extracted from the train of stimulation's first laser pulse, and
194 the following 6 s window was analyzed to find out if the mice initiated a licking behavior at any of the
195 3 sippers. Then, we built a two-dimensional array containing the probability of licking any sipper given
196 the mouse's distance and angle during the first laser of each opto-stimulation train.

197

198 *Closed-loop stimulation task*

199 The next eleven sessions, animals were tested in the same operant conditioning chamber described
200 above, but this time opto-self-stimulation was delivered when the subject made a head entry in the
201 central port (containing a sipper filled with water). The laser was turned on by 2 s with a time out of 4
202 s post-stimulation. Lateral ports delivered sucrose 3 and 18%. After this and on subsequent days, the
203 central port stimulus was replaced across sessions following the protocols described below.

204 Table 2. Closed-loop stimulation protocol

Stimuli in central port	**Sessions tested**
Water	Last 5 sessions of the closed-loop (Figure 7)
Extinction (No opto-stimulation)	4
Water	3
Empty sipper	3
Water	3
0.004% Quinine	4
Airpuff	4
Unavoidable airpuff	3
Sucrose 18% (Water was placed in the sucrose 18% port)	4

205

206 *Closed-loop stimulation task (one single bottle test: quinine)*

207 Mice were put in a custom-made box with 18 x 13 x 7.5 cm internal dimensions. The front wall was
208 equipped with one single sipper (a contact lickometer with V-shape registered individual licks).
209 0.004% quinine or 18% sucrose were tested with sated and water-deprived mice during 3 and 2
210 sessions, respectively. Opto-self-stimulation (2 s on with a time out of 4 s) was delivered when mice
211 made a head entry in the central port. Water-deprived mice had access to *ad libitum* water for 1 h after
212 the session finished.

213

214 *Open loop stimulation in an open field with Chow, high-fat diet, or granulated sugar cube*

215 Animals were placed in the circular arena's center (50 cm of diameter). Three or two food plates were
216 equidistant to each other, and each contained either Chow, high-fat diet, or granulated sugar cube. Mice
217 were opto-stimulated by alternating 5 min block with no-laser and 5 min laser block across the session.
218 In open loop, the laser was turned "on" regardless of the mice's behavior and spatial position in the
219 arena. All sessions were recorded and analyzed with bonsai software (https://open-ephys.org/bonsai).
220 We calculated the mouse' centroid at each frame and used that information to create a heatmap of its
221 position. The distance of the mouse's centroid from each stimulus was computed. An interaction
222 occurred when the distance was below 60 mm, and the animal stayed there for at least 1 s. Food plates
223 were weighted at the beginning and the end of each session.

224

225 *Closed-loop in an open-field*

226 In a circular arena, four stimuli were located equidistant to each other, either wood cork, Chow,
227 chocolate pellets, or a sipper filled with a 10% sucrose solution. During the session, a homemade
228 computer vision program tracked in real-time the position of the subject. Each mouse needs to enter
229 the designated area to receive opto-self-stimulation (2 s laser on and 4 s off). Mice need to leave and
230 re-enter the designated area to begin a new trial.

231

232 *Brief access test*

233 To evaluate sucrose's palatability, we used a brief access test in water-deprived mice. For this task, we
234 used a licking spout consisting of independent stainless-steel needles (20-gauge) cemented together
235 with dental acrylic at the sipper tube's tip [29]. Each needle was connected to a solenoid valve (Parker,

236 Ohio, USA) by a silicon tube. The drop (~2 µL) was calibrated before each session and maintained by
237 using a pressurized control system. The sequence of a trial is as follows. At the beginning of the task,
238 the sipper is extended in a lick position. To start a new trial, the subject had to introduce its head into
239 the central port to turn on the laser, then elicited a dry lick to start the reward epoch (7s). During this
240 period, a tastant's drop was delivered every lick. Once the epoch was finished, the sipper was retracted
241 for 3 s as inter-trial interval, and then the sipper was re-extended into the central port. Tastant solutions
242 (water, sucrose 3%, and sucrose 18%) were delivered in a semi-random order. The laser was turned on
243 using a closed-loop protocol. Briefly, each head entry triggers the laser on for 2s (or 7s). The time of
244 stimulation changed between sessions, either 2 s or 7s, in order to test whether licking could be evoked
245 for a more extended period. At the end of the session, mice had access to *ad libitum* water for 1 h.
246 Protocols are described below:

247 Table 3. Brief access taste protocol

Laser on	Time on	# Sessions
All trials	2 s	6
Water trials	2 s	3
Sucrose 3% trials	2 s	3
Sucrose 18% trials	2 s	3
All trials	7 s	4
Water trials	7 s	3
Sucrose 3% trials	7 s	3
Sucrose 18% trials	7 s	3
Mock laser (sucrose 3% trials) *	7 s	3

248 *For mock laser, mice were connected to a false fiber optic, whereas the real laser was glued outside
249 the skull to emit blue light.

250

251 In addition, in the same behavioral box, a brief access test was performed while the LHA was recorded,
252 followed by optogenetic tagging in the same session. Tastant solutions (artificial saliva, water, sucrose

253 3%, and 18 %) were delivered in a semi-random order. We operationally defined sucrose's palatability
254 as the enhancement of hedonically positive oromotor responses evoked by increasing sucrose
255 concentrations [30,31].

256

257 *Electrophysiology*

258 Neural activity was recorded using a Multichannel Acquisition Processor System (Plexon, Dallas TX,
259 USA) interfaced with Med Associates to record behavioral events simultaneously [32]. Extracellular
260 voltage signals were first amplified by an analog head-stage (Plexon, HST/16o25-GEN2-18P-2GP-
261 G1), then amplified and sampled at 40 kHz. Raw signals were band-pass filtered from 154 Hz to 8.8
262 kHz and digitalized at 12 bits resolution. Only single neurons with action potentials with a signal to
263 noise ratio of 3:1 were analyzed [32]. Action potentials were isolated online using a voltage-time
264 threshold window and three principals' components contour templates algorithm. Furthermore, off-
265 line spike sorting was performed (Plexon, offline sorter), and only single units with stable waveforms
266 across the entire session were included in the analyses [32].

267

268 *Neuronal classification*

269 Laser activated neurons ($pLHA^{Vgat}$) were detected by using two methods: 1) a Kruskal-Wallis to
270 compare firing rates during a baseline (-1 to -0.04 s), against the activity during the presentation of
271 laser (0 – 2 s, aligned to laser onset). 2) Cumsum statistic [33] to obtain the first bin (1 ms resolution)
272 after the first laser pulse that significantly increased the firing rate above baseline (from -20 to 0 ms).
273 Only neurons showing a significant value in both tests were considered laser-activated $pLHA^{Vgat}$.

274

275 We used a Kruskal-Wallis test to compare firing rates during the baseline (-1 to -0.04 s) period, against
276 the activity during the presentation of laser (0 to 2 s) aligned to laser onset for all frequency tested.
277 Neurons that significantly increased their firing rate during the laser stimulation were named
278 "Activated," and neurons that decreased their activity were named "Inhibited" or non-LHA^{Vgat} neurons.
279 Neurons with no significant modulation were classified as "unmodulated."

280

281 *Optotagging stimulation protocol*

282 To identify LHA^{Vgat+} neurons related to sucrose's palatability once the brief access test was finished,
283 each mouse with an optrode was tested in the optotagging task, and the laser was turned on 2 s at 50
284 Hz. ChR2-expressing cells LHA^{Vgat+} were those with an action potential evoked within ≤ 15 ms latency
285 [34], as measured by a cumsum statistic described in [33].

286

287 *Palatability-responsive neurons*

288 We used a best-window analysis to identify neurons whose firing rate correlated with palatability-
289 induced oromotor responses, following a previous study [29]. This method has been used to detect
290 palatability-related activity in a brief access test. Briefly, during each recording session, a palatability-
291 index (PI) was calculated. The PI reflects the overall appetitive oromotor responses elicited by each
292 tastant delivered in the session. It was computed by averaging the lick rate (number of licks/ 7s) during
293 the entire reward epoch, including all the trials per session. In mice, the PI takes values between 0-8
294 Hz for sucrose stimuli [35]. 0 Hz means animals ultimately rejected a solution in all trials, whereas 8
295 Hz indicates, they licked continuously during the entire reward epoch, thus reflecting a greater
296 palatability response elicited by the tastant. Then, the firing rate was calculated for a variety of time

297 centers (from 0.25 to 6.75 s with 0.5 s steps), and multiple window sizes (from 0.5 to 7 s, 0.5s steps),
298 such that each window was estimated as the center ± (window size/2). We identified the windows
299 where the mean firing rate was significantly different for at least one tastant delivered (i.e., tastants,
300 using a Kruskal-Wallis test at an alpha of 0.05). Next, we computed Pearson's correlation coefficient
301 (r; the alpha level at 0.05) between both the PI and the firing rate on a trial-by-trial basis. The window
302 with the largest absolute Pearson's correlation coefficient was selected as the "best-window." Thus,
303 for the "best-window" and each statistical test (i.e., Kruskal-Wallis test and Pearson's correlation
304 coefficient), a permutation assay was used for multiple-testing correction. This analysis was
305 accomplished by shuffling the different tastant delivered 20,000 times (using the Matlab function
306 "shuffle"). A corrected *p*-value was obtained using the following formula $p = (k+1)/(n+1)$, where k is
307 the times in which a permuted distribution leads to a *p*-value smaller than the original *p*-value and n is
308 the number of repetitions. Only time-windows with *p*'s < 0.05 in both tests (Kruskal-Wallis and
309 Pearson Correlation) were considered as statistically significant. Thus, the "best-window" is where the
310 firing rate maximally correlated with the oromotor responses elicited by sucrose's palatability on a
311 trial-by-trial basis. Results were qualitatively similar if we used the lick bout duration rather than the
312 lick rate to compute the PI (data not shown) [29].

313

314 *Data Analysis*

315 Data analysis was performed using MATLAB (The MathWorks Inc., Natick, MA) and GraphPad Prism
316 (La Jolla, CA, USA). We used the mean ± sem and the α level at 0.05.

317 **Results**

318 Initially, we determined the optimal stimulation parameters to activate LHA GABAergic neurons. This
319 was accomplished by implanting an optrode in naïve mice that constitutively expressed ChR2 in

320 GABAergic neurons expressing the gene for the vesicular γ-aminobutyric acid transporter (VGAT-
321 ChR2 mice) [36] (Figure 1A-B). We found that a laser stimulation of 50 Hz (10 ms width) evoked the
322 strongest LHA neuronal responses (Figure 1C-F) [37]. Unless otherwise mentioned, this frequency
323 was used for all subsequent experiments.

324

325 *LHA neurons encode sucrose's palatability*

326 In rats, previous electrophysiological studies suggest that ensembles of LHA neurons process
327 palatability related information [17,18,38,39]. Based on these results, we then asked whether LHA
328 neurons could provide information about sucrose's palatability by using a behavioral task with only
329 palatable stimuli (i.e., artificial saliva (AS), water, sucrose 3 wt%, and sucrose 18 wt%). We
330 operationally defined sucrose's palatability as the enhancement of hedonically positive oromotor
331 responses triggered by increasing sucrose concentrations [29–31]. Specifically, oromotor responses
332 include an increase in the lick rate or bout size. Thus, this definition of palatability should not be
333 confused with a conscious hedonic feeling of pleasant taste that humans experience [40,41]. To this
334 end, taste responses were recorded from a total of 284 LHA neurons, while VGAT-ChR2 mice
335 performed a brief access test (Figure 2A). To uncover palatability-responsive neurons, we analyzed
336 neuronal activity using a previously described "best-window analysis" [29] (see Materials and
337 Methods). This strategy detects the optimal interval, where the firing rate best correlates with the
338 sucrose's palatability index (PI) computed as the average lick rate, on a session by session basis, evoked
339 by each gustatory stimulus in the Reward epoch (Figure 2B). Figure 2C depicts the responses of two
340 representative LHA neurons: as expected, we found one whose activity increased as the sucrose
341 concentration increased (positive Pearson's correlation, r = 0.87; Figure 2C *left*), and the other was
342 negatively associated with palatability oromotor responses evoked by sucrose (r = -0.64; Figure 2C

343 *right).* Figure 2D shows the normalized activity exhibiting either positive (59/284 neurons, 21%) or
344 negative correlations (76/284, 27%) with the PI. Thus, these data confirmed that the LHA mice's
345 neurons exhibit palatability-related responses, and this activity can be either correlated or anti-
346 correlated with the sucrose solution's PI.

347

348 *Dynamic tracking of palatability over the entire course of a behavioral session*

349 Having demonstrated that LHA neurons encode sucrose's palatability, we then explored whether LHA
350 palatability-related neurons can dynamically adjust their responses to track the changes in sucrose's
351 palatability across the session when the animals would approach satiation. We found that the lick rate
352 declined across the session as a function of sucrose's palatability (Figure 2E [RM ANOVA, main effect
353 of stimuli $F_{(3, 402)} = 163.7$, $p < 0.0001$,effect of time $F_{(9, 1206)} = 100.4$, $p < 0.0001$]), and significant
354 stimuli by time interaction $F_{(27, 3618)} = 16.54$, $p < 0.0001$]). Briefly, early in the session, animals licked
355 more for all stimuli, but as the session progressed, the lick rate declined especially for AS and water
356 but not for sucrose (3% and 18%), indicating that they tracked palatability responses rather than satiety
357 (Figure 2E). Similar to what has been found in the Nucleus Accumbens Shell (NAcSh) [29], a brain
358 region that sends outputs to LHA and is involved in feeding and palatability [29,42], we also found
359 that the LHA neuron's firing rate (either increasing or decreasing neurons) adjust across the session to
360 reflect sucrose's palatability (Figure 2F). These data indicate that whithin the session as the animals
361 approach satiety, the responses of the Palatability related-neurons tracked the rapid decline in the lick
362 rate mainly for the two less palatable stimuli (i.e., AS and water) but not for the higher sucrose-
363 concentration (sucrose 3% and 18%), suggesting these neurons are tracking palatability and not satiety.

364

365 *A subpopulation of opto-identified LHA^{Vgat+} neurons encodes sucrose's palatability*

366 To identify LHA^{Vgat+} neurons from our recordings, we opto-stimulated the same mice recorded in the
367 brief access test seen in Figure 2. We verified the stability of the waveforms between tasks (i.e., brief
368 access test and optotagging), and thus we only included single units with stable waveforms in the
369 analysis (Supplementary Figure 1). Figure 3A displays the setup and the normalized (Z-score) activity
370 of laser-activated neurons (48%; 137/284) (for details, see Material and Methods). Since these neurons
371 may include ChR2 expressing cells and other LHA neurons modulated by indirect polysynaptic
372 feedback of afferent fibers from other areas in the brain [43], we decided to name them putative
373 LHA^{Vgat} (pLHA^{Vgat}) neurons. Note that pLHA^{Vgat} neurons comprise the ensemble recruited by the
374 optogenetic stimulation of LHA GABAergic neurons, suggesting they convey similar information.
375 Therefore, we next evaluated whether pLHA^{Vgat} neurons were correlated with sucrose's palatability.
376 In total, 50% (69/137) of laser-activated neurons exhibited responses that were significantly
377 palatability related; specifically, 34% showed a positive correlation (46 out of 137), whereas 17% (23
378 out of 137) had a negative correlation with sucrose's palatability (Figure 3B, Positive vs. Negative chi-
379 square test $_{(1, 274)} = 10.25$, $p < 0.01$). Figure 3C shows the population activity of pLHA^{Vgat} neurons with
380 either a positive (yellow) or negative (purple) correlation with the PI (red). Furthermore, from all
381 recorded LHA neurons that encode sucrose palatability with a Positive correlation (n = 59, see Figure
382 2D), we found that more than 78% (46/59) belonged to the pLHA^{Vgat} (Figure 3D). In contrast, only
383 30% (23/76) of pLHA^{Vgat} neurons were Negative palatability related (Figure 3D, Positive vs. Negative
384 chi-square test $_{(1, 135)} = 30.25$, $p < 0.0001$). Thus, pLHA^{Vgat} tends to encode sucrose's palatability with
385 a biased towards positive correlations.

386 To confirm the identity of LHA^{Vgat+} neurons, we searched for neurons in which a brief pulse of light-
387 evoked an action potential with an early latency (< 15 ms), that would reflect the expression of ChR2
388 in their somas [34]. From the pLHA^{Vgat} population, in total, 52 % (71 / 137) neurons exhibited an early

389 response to blue light (Figures 3E-F), suggesting that these pLHA^{Vgat} neurons were LHA^{Vgat+} neurons.
390 We found that over half of the identified LHA^{Vgat+} neurons, 55% (39/ 71), were involved in encoding
391 sucrose's palatability, and the remaining (45%) were unmodulated by sucrose. From the LHA neurons
392 related to sucrose's palatability, 31% of LHA^{Vgat+} neurons positively correlated with sucrose's
393 palatability (22/71), and 24% were anticorrelated (17/71) (Figure 3G, Positive vs. Negative; n.s.). The
394 LHA^{Vgat+} neuronal responses with positive and negative correlations with lick-related palatability
395 responses are seen in Figure 3H. Once again, we compared the proportion of opto-identified LHA^{Vgat+}
396 neurons against all palatability-responsive neurons recorded in the LHA. We found a trend to encode
397 sucrose's palatability in a positive, rather than negative manner. That is, 37% (22/59) of LHA^{Vgat+}
398 neurons belonged to the Positive palatability-related population, whereas only 22% (17/76) were
399 Negative palatability-related neurons (Figure 3I, Positive vs. Negative; n.s.). Altogether, these data
400 suggest that LHA^{Vgat+} neurons tend to encode sucrose's palatability in a positive rather than in a
401 negative manner. More important, our data are in agreement with the idea that the LHA^{Vgat+} neurons
402 comprise many heterogeneous subpopulations with different functional responses [22].

403

404 *Non-LHA^{Vgat} neurons negatively encode sucrose's palatability*

405 We also found that 25% of LHA neurons exhibited a laser-induced inhibition (70/284, non-LHA^{Vgat}
406 neurons, Figure 3J), and the remaining 27% (77/284) were unmodulated during blue light stimulation
407 (Figure 3J, black trace). Unlike pLHA^{Vgat} neurons, only 7% (5 out of 70) of the non-LHA^{Vgat} neurons
408 showed a positive correlation, whereas the vast majority 36% (25 out of 70), had a negative correlation
409 with sucrose's palatability (Figures 3K and 3L, Positive vs. Negative chi-square test $_{(1, 140)} = 16.97$, p
410 < 0.0001). These results suggest that non- LHA^{Vgat} neurons (perhaps glutamatergic Vglut2 neurons)

411 preferentially encode sucrose's palatability with negative correlations (Figure 3M, Positive vs.
412 Negative chi-square test $_{(1, 135)} = 11.46$, $p < 0.001$).

413

414 *Activation of LHA^{Vgat+} neurons drives sucrose intake*

415 If a subpopulation of LHA GABAergic neurons preferentially encodes sucrose's palatability by
416 increasing firing rates, its optogenetic stimulation should promote increased sucrose intake. To
417 characterize its impact on sucrose intake, we used an open loop optogenetic stimulation involving 5
418 min blocks with laser and no-laser stimulation, while naïve VGAT-ChR2 mice had *ad lib* access to a
419 sipper filled with sucrose 10% (Figure 4*A*). We analyzed the intake as a function of laser frequency
420 and found that in the first three blocks with laser, 50 Hz stimulation induced a significant increase in
421 sucrose intake (Figure 4B; Blocks 2, 4, and 6) compared with the previous blocks of no-laser (Figure
422 4*B;* $p < 0.001$; Blocks 1, 3, and 5). Figure 4*C* shows a raster plot for licking responses of a
423 representative open loop session. At 50 Hz, we found that feeding (licking) was elicited within a 0.72
424 s ± 0.03 latency from laser onset, and it abruptly stopped (0.27 s ± 0.1) after laser offset (see blue dash
425 rectangles). VGAT-ChR2 mice exhibited an increase in the laser-bound feeding index (number of licks
426 in a 2.5 s window from laser onset divided by total licks in the session; hereafter named laser-bound
427 feeding) as the laser frequency increased (Figure 4*D;* two-way ANOVA, group by frequency
428 interaction; $F_{(5, 36)} = 12.86$, $p < 0.0001$). Thus, to induce sucrose intake, a subset of LHA^{Vgat+} neurons
429 requires continued activation. Our data then confirmed that 50 Hz is the best stimulation frequency to
430 drive neuronal responses and sucrose intake.

431

432 *LHA^{Vgat+} neurons do not induce a persistent hunger state*

433 A previous study showed that brief optogenetic stimulation of "hunger-inducing" AgRP neurons before
434 food availability promotes consummatory behavior that persists for several minutes in the absence of
435 continued AgRP neuron activation [44,45]. Based on this study, we tested whether the pre-stimulation
436 of LHA^{Vgat+} neurons could evoke a similar hunger state. Unlike AgRP neurons [44,45], pre-stimulation
437 of LHA^{Vgat+} neurons failed to evoke and sustain subsequent sucrose intake (see Supplementary Figure
438 2). Our results suggest that feeding occurs while LHA^{Vgat+} neurons are active (Figure 4C), but they do
439 not induce a persistent hunger state as AgRP neurons do [45].

440

441 *Open loop activation of LHA^{Vgat+} neurons drives intake of the highest sucrose concentration available*

442 To test whether activation of LHA^{Vgat+} neurons promotes the intake of the most palatable available
443 stimuli, naïve WT and VGAT-ChR2 mice were opto-stimulated in an open loop protocol, with access
444 to three adjacent ports containing water, sucrose 3%, or sucrose 18% (Figure 5A). As expected, both
445 WT and VGAT-ChR2 mice preferred sucrose 18% over water and sucrose 3% (Figure 5B, [WT: two-
446 way ANOVA main effect tastants; $F_{(2, 1560)} = 543.3$, $p < 0.0001$; VGAT-ChR2: $F_{(2, 3144)} = 983$, $p <$
447 0.0001]). However, we found that during laser stimulation, sated VGAT-ChR2 mice increased their
448 intake of 18% sucrose but mainly during the laser-activated blocks compared with controls (Figure 5B-
449 *right* [two-way ANOVA group by laser block interaction $F_{(7, 1568)} = 31.86$, $p < 0.0001$]) and rarely
450 licked in the absence of stimulation (Figure 5C). In this regard, VGAT-ChR2 mice seem to counteract
451 the evoked sucrose intake by voluntarily restraining consumption in no-laser blocks (Blocks 3, 5, and
452 7), resulting in no significant differences between groups in the total intake of 18% sucrose (Figure
453 5C, see black squares, unpaired Student's t-test, $t_{(196)} = 1.512$, $p = 0.1320$). A between days analysis
454 revealed that the evoked 18% sucrose intake began from the first stimulation day (Figure 5D [RM
455 ANOVA laser blocks, $F_{(1, 22)} = 64.64$, $p < 0.0001$]), although sucrose consumption ramps up

456 throughout the days (Figure 5D [RM ANOVA main effect days, $F_{(10, 220)} = 2.169$, $p < 0.05$]). This
457 suggests that LHA^{Vgat+} neurons, rather than inducing hunger *per se*, induced a learning process that
458 potentiates the intake of the most palatable stimulus and confines consumption mainly in the presence
459 of opto-stimulation.

460

461 The small increase in water and sucrose 3% intake observed during opto-stimulation of LHA^{Vgat+}
462 neurons could be explained by random stimulation near those tastants (Figure 5B *right panel*).
463 Accordingly, we found in laser blocks 2, 4, and 6, a significant increase in water and sucrose 3% in the
464 VGAT-ChR2 mice compared with the WT mice that completely neglected those tastants (Figure 5B,
465 ^ $p < 0.05$ for sucrose 3%; † $p < 0.05$ for water). We hypothesize that this additional intake can be
466 attributed to trials where the laser-activation occurred near these less palatable stimuli. To answer this,
467 we employed a videography analysis (Figure 6A-B). When opto-stimulation occurred in the distance
468 minor to 50 pixels (approximately 3 cm, see Materials and Methods) relative to water or sucrose 3%
469 ports, the licking probability increased significantly after opto-stimulation (Figure 6B). The angle of
470 the head was less informative (Figure 6C-D). Conversely and since mice are naturally attracted to the
471 most palatable tastant, they spent more time near the lateral port with 18% sucrose, increasing their
472 overconsumption (Figure 6C, Video 1). Moreover, we observed that for the sucrose 18% port, even
473 when the mouse position was twice as far (i.e., 6 cm) from sucrose 18% port, the licking probability
474 increased significantly. These data are consistent with a study showing that opto-stimulation of
475 LHA^{Vgat+} neurons promotes the intake of the nearest stimulus [24] but further demonstrates that the
476 most palatable stimulus has nearly twice the distance of attraction than the other less palatable options.

477

478 *Open loop activation of LHA^{Vgat+} neurons also increases the time spent and drives the intake of the*
479 *most palatable solid food available*

480 We also explored whether LHA GABA neurons could induce the intake of the most palatable solid
481 food available. Thus, using an open loop protocol, we opto-stimulate these neurons while mice choose
482 among different solid foods. We found that optogenetic activation of LHA^{Vgat+} neurons increased the
483 time spent near the most palatable food available. Mice spent more time near the high-fat diet than the
484 granulated sugar cube or the Chow food pellet (see Supplementary Figure 3 and Video 2). When mice
485 were able to choose between a sugar cube and a Chow pellet, activation of these neurons increased the
486 consumption of sugar cube over Chow (see Supplementary Figure 4 and Video 3). Our data suggest
487 that open loop stimulation of LHA GABAergic neurons promotes the intake of the most palatable food
488 available.

489

490 *Closed-loop stimulation of LHA^{Vgat+} neurons drives the intake of the nearest appetitive stimuli*

491 To further test the idea that LHA^{Vgat+} neurons could induce preference to a proximal (but less palatable)
492 stimulus over a distal one with higher hedonic value, we used a closed-loop stimulation protocol. That
493 is, the same mice (from Figure 5) were photostimulated, but here the laser was triggered by each head
494 entry in the central port (i.e., opto-self-stimulation). This closed-loop configuration guarantees that
495 stimulation only occurs proximal to water, the least palatable stimulus of the three in the box (Figure
496 7*A-right*). We found that activation of LHA^{Vgat+} neurons is rewarding since transgenic mice visited the
497 central port significantly more and performed a higher number of opto-self-stimulations than the WT
498 mice (Figure 7B, unpaired Student's t-test, $t_{(196)} = 12$, $p < 0.0001$). Surprisingly, the total number of
499 licks in the session seen in Figure 7C shows that during closed-loop stimulation, the VGAT-ChR2 mice
500 explored and consumed more water than the WT mice. Note that in both open loop and closed-loop

501 protocols, the WT and VGAT-ChR2 mice exhibited, at the end of the session, a similar number of licks
502 for 18 wt% sucrose (Figure 7C [two-way ANOVA group by protocol interaction $F_{(1, 391)} = 2.172$, $p =$
503 0.1414]). That is, the total licks for sucrose 18% were not significantly different between groups,
504 suggesting that these neurons do not interfere with the overall attractiveness of sucrose. However, by
505 counting the number of licks given when the laser was turned on (in a 2.5 s window from laser onset-
506 see Figure 7D), we uncovered a striking change in preference. As noted, in the open loop, the VGAT-
507 ChR2 mice exhibited a higher preference to sucrose 18 wt%, over both sucrose 3 wt% and water. Now,
508 in the closed-loop protocol, the same transgenic mice consumed more water compared with WT ($p <$
509 0.0001), and the consumption of water was about the same as sucrose 18% ($p = 0.8731$, n.s.; Figure
510 7D). The increase in water intake was selective to the photostimulation window since the transgenic
511 mice only drank sucrose 18%, and neglected water when the laser was turned off (see arrow Figure 7E,
512 $p < 0.0001$). Thus, LHA^{Vgat+} neurons could promote water intake, but only when it is the nearest
513 stimulus. The sucrose preference index (Figure 7F) showed that during the open loop all VGAT-ChR2
514 mice preferred sucrose 18% over water (Figure 7F; values > 0.5 and near to 1), whereas in the closed-
515 loop protocol, when water was the nearest stimulus, most mice (n = 9 out of 12), significantly
516 diminished their sucrose preference (Figure 7F, see the drop in preference index; paired Student's *t*-
517 test, $t_{(58)} = 7.98$, $p < 0.0001$). From these 9 animals, 6 exhibited a higher preference to water over
518 sucrose 18% (Preference index values < 0.5; Video 4). Figure 7G shows the color-coded location of
519 fiber optic tips in each VGAT-ChR2 mice plotted in Figure "7F." However, the location of the optical
520 fibers does not explain the variability in preference. Perhaps variability is due to different behavioral
521 strategies used by each mouse. Nevertheless, the large variability in the drop of sucrose's preference
522 resembles the findings with sweet-induced facilitation by electrical ICSs [9]. These data suggest that
523 LHA^{Vgat+} neurons drive consummatory behavior by integrating the proximity and the hedonic value of
524 the stimulus.

525

526 *After repeated stimulation, the correlation between laser-bound feeding and self-stimulation*
527 *strengthens*

528 Previous studies have shown that after repeated LHA bulk stimulation (either electrically or with
529 optogenetic targeting all cell-types together), subjects switched from exhibiting stimulus-bound
530 feeding to only self-stimulating, indicating that LHA evoked feeding and reward could represent two
531 distinct processes [37,46]. Consequently, we explored whether laser-bound feeding changed after
532 repeated optogenetic stimulation. In contrast to previous studies, we observed that laser-bound feeding
533 induced by LHA^{Vgat+} neurons strengthened across sessions (Figure 8A, First 3 days: $r = 0.12$, $p = 0.69$;
534 Last 5 stimulation days: $r = 0.63$, $p < 0.05$) and after repeated stimulation, both opto-self-stimulation
535 and laser-bound feeding exhibited a robust correlation (Figure 8B, First 3 days: $r = 0.42$, $p = 0.16$; Last
536 5 days: $r = 0.61$, $p < 0.05$), suggesting that LHA evoked-feeding (licking) involves a learning process
537 [47] and that LHA GABAergic neurons are a common neural substrate for feeding and reward.

538

539 *The "stimulus-proximity effect" is not restricted to liquid tastants, and it also occurs with chocolate*
540 *and Chow pellets*

541 The "proximity effect" evoked by LHA^{Vgat+} neurons was not restricted to liquid tastants, it also applied
542 to solid foods. In a real-time place preference arena with four stimuli (Figure 9A), when chocolate
543 pellets or Chow food were the designated foods near opto-self-stimulation of LHA^{Vgat+} neurons, mice
544 also increased the time spent near those foods (Figure 9B; Video 5) as well as their intake (Figure 9C).
545 Thus, these LHA GABAergic neurons reinforced the approach and exploration to any, if not the most
546 appetitive stimuli, that happened to be proximal to the opto-stimulation.

547

548 *LHA^{Vgat+} neurons activation is rewarding*

549 In the same WT and VGAT-ChR2 mice tested in the closed-loop configuration seen in Figure 7, we
550 went on to show that mice visited the central water-port to opto-self-stimulate. To do this, we
551 performed extinction sessions with the laser disconnected (Figure 10A). We observed a rapid decrease
552 in the number of opto-self-stimulations (Figure 10B; Extinction phase, gray shadow). As expected,
553 self-stimulation rapidly recovered when the laser was turned on again (Figure 10, see water after
554 extinction). Thus, LHA^{Vgat+} neurons convey a hedonically positive, rewarding signal [22].

555

556 *LHA^{Vgat+} neurons also promote licking an empty sipper*

557 A previous study demonstrated that chemogenetic activation of LHA^{Vgat+} neurons increased gnawing
558 to non-edible cork [23]. In the absence of other stimuli but cork, we also observed gnawing behavior
559 in some mice, although we did not systematically study stereotypy (see Video 6). Instead, we further
560 explored this idea by replacing water, in the central port, with an empty sipper (Figure 10, Empty
561 sipper). Transgenic mice continued opto-self-stimulating at the same place as if water were still present
562 in the central port. LHA^{Vgat+} stimulation evoked licking an empty sipper compared with WT mice
563 (Figure 10C, unpaired Student's t-test, $t_{(40)} = 2.532$, $p < 0.05$). Thus, LHA^{Vgat+} neurons evoke an
564 imminent urge to express consummatory behavior even in the form of dry licking an empty sipper, a
565 non-biological relevant stimulus. This effect is perhaps mediated by an increase in the rewarding value
566 of appetitive oromotor responses *per se*.

567

568 *When sucrose is available, activation of LHA^{Vgat+} neurons neither promotes liquid intake of an*
569 *aversive bitter tastant nor tolerance of punishment, but it further increases sucrose consumption*

570 To explore whether the "stimulus-proximity effect" was also applied to aversive stimuli, we replaced
571 the central stimulus (water) with aversive stimuli, including quinine or airpuffs (Figure 10*A*). Upon
572 quinine presentation, the number of licks given in the central port sharply decreased (Figure 10C,
573 green), but transgenic mice continued to self-stimulate and go to the lateral port to lick for sucrose 18%
574 (Figure 10D, green). During the airpuff delivery phase (Figure 10D, dark gray), we obtained similar
575 results than those in quinine stimulation. Next, we required the animal to lick, at least once, the central
576 sipper to trigger opto-stimulation (thus making the airpuffs unavoidable). Under this condition,
577 transgenic mice completely stopped self-stimulation (Figure 10B, cyan) and aborted 18% sucrose
578 intake from the lateral port (Figure 10D, cyan). These results suggest that, in sated mice, LHA^{Vgat+}
579 neurons did not induce quinine intake nor increase tolerance to airpuffs.

580

581 Finally, we explored whether proximity to the most palatable tastant further facilitated its
582 overconsumption. Thus, we exchanged the position of water and sucrose 18%. When sucrose 18% was
583 delivered in the central port, transgenic mice greatly overconsumed it (Figure 10C, pink). The intake
584 of sucrose 18% was higher than for all the other tastants tested previously ($p < 0.0001$). These results
585 collectively suggest that activation of LHA^{Vgat+} neurons is rewarding and promotes increased
586 consumption of the nearest stimulus even if it is not the most palatable (e.g., water and empty sipper).
587 If the nearest stimulus happens to be the most palatable (i.e., sucrose 18%), then LHA GABA neurons
588 further facilitated its consumption.

589

590 *LHA GABA neurons increased quinine intake but only in water-deprived mice*

591 Having demonstrated that in the presence of sucrose, activation of these neurons failed to increase
592 quinine intake (Figure 10C green), with a new group of naïve mice, we then explored whether LHA^{Vgat+}
593 neurons could induce quinine intake when it was the only option. As expected, in sated mice, we found
594 that activation of LHA^{Vgat+} neurons did not affect quinine intake compared with WT (Figure 11A).
595 Surprisingly, it promoted a higher quinine intake when transgenic mice were water-deprived (Figure
596 11B, unpaired Student's t-test, $t(16) = 3.623$, $p < 0.01$), specifically during photostimulation window
597 (Figure 11B, unpaired Student's t-test, $t(16) = 5.821$, $p < 0.0001$), suggesting that activation of these
598 neurons is sufficient to increase the acceptance of bitter tastants but only during water deprivation. In
599 contrast, we found that regardless of homeostatic needs, activation of these neurons increased sucrose
600 18% intake relative to WT mice (Figure 11C-D).

601

602 *Activation of LHA^{Vgat+} neurons enhances palatability*

603 We next explored whether, at equal stimulus distance, these neurons could enhance palatability
604 responses. To do this, in a new group of water-deprived mice, we employed a brief access test again.
605 In this task, we delivered gustatory stimuli water, sucrose 3%, and sucrose 18% from the same sipper
606 tube, but in different trials. Figure 12*A* displays the trial's structure (same conventions as in Figure 2).
607 We found that WT mice increased their licking rate as a function of sucrose's concentration, reflecting
608 its palatability (Figure 12B, *left panel*). In contrast, during the 2 s of laser stimulation, the VGAT-ChR2
609 mice exhibited a greater lick rate for all three tastants. However, after the laser was turned "off," these
610 mice abruptly stopped licking for water and sucrose 3% (Figure 12*B, right panel*) compared with the
611 WT group. Moreover, when stimulation was paired with water trials, transgenic mice selectively
612 increased their lick rate to water (Figure 12C, blue line and arrow), even surpassing licking responses

613 evoked by the most palatable sucrose 18%. A similar enhancement of oromotor responses was
614 observed by pairing sucrose 3% trials with LHA^{Vgat+} opto-self-stimulation (Figure 12D, pink).
615 Likewise, the laser-bound feeding (licking rate) was strongest when sucrose 18% was paired with the
616 optogenetic stimulation (Figure 12E, red, see arrow).

617

618 Finally, we show that palatability responses could be artificially extended as long as LHA^{Vgat+} neurons
619 were continuously activated. For this, we photostimulated them for up to 7 s. We observed a similar
620 enhancement pattern, maintained for the duration of opto-stimulation (see Figure 12F-I see arrows),
621 suggesting that LHA^{Vgat+} neurons can adjust the enhancement of oromotor palatability responses by
622 simply sustaining its neuronal activity. We verified that using optrode recordings, that 7 s optogenetic
623 stimulation produced sustained LHA^{Vgat+} neuronal responses (Figure 12J). Moreover, transgenic mice
624 did not merely use the light as a cue to guide behavior since laser-stimulation with a mock optical fiber
625 failed to increase licking (Figure 12K). In sum, our data demonstrate that activation of LHA^{Vgat+}
626 neurons triggers a reinforcing signal that amplifies the positive hedonic value of proximal stimuli,
627 promoting overconsumption.

628

629 **Discussion**

630 LHA has historically been viewed as a critical center for feeding [1–3], although it also processes
631 sucrose's palatability related information [18,38,48]. In addition to caloric value, sucrose's palatability
632 is the affective or hedonic attribute of sweetness that determines whether to like it or not. Despite the
633 importance of palatability to promote overconsumption, the specific LHA cell-type(s) identity involved
634 in processing sucrose's palatability has remained elusive. Our results demonstrated that a
635 subpopulation of LHA^{Vgat+} GABAergic neurons encodes sucrose's palatability by exhibiting two

636 opposite modulatory patterns, either correlating positively or negatively with the palatability index,
637 with a bias towards a positive correlation. Furthermore, opto-stimulation of LHA^{Vgat+} cell somas
638 promoted approach and intake of the most salient available and palatable tastant. In contrast, opto-self-
639 stimulation promoted increased liquid intake of the less-attractive and proximal stimuli, despite having
640 more palatable but distal tastants available. These findings show that LHA^{Vgat+} neurons compute and/or
641 combine, at least, two types of information: one related to stimulus proximity and the other to
642 palatability that results in enhancing stimulus-saliency [24]. More important, these data uncovered a
643 new function of a subgroup of LHA^{Vgat+} neurons as physiological potentiators of sucrose's palatability.

644

645 Previous work has shown that LHA^{Vgat+} population contains many subpopulations with different
646 functional responses, with at least one ensemble responding to appetitive (approach) and other to
647 consummatory behaviors [22]. Furthermore, activation of these neurons is rewarding, induces
648 voracious eating [22,23], and promotes interaction of the nearest stimuli (either objects or other mice)
649 [24], suggesting that they play a role in multiple motivated behaviors. However, it is also known that
650 LHA connects and receives direct inputs from multiple cortical and subcortical gustatory regions [10–
651 13,49], and some electrophysiological studies report that LHA neurons respond to gustatory stimuli –
652 in particular to tastant palatability [16,17,38,48,50]. As noted, in rodents, palatability is operationally
653 defined as the enhancement of hedonically positive oromotor responses induced by stimulating the
654 tongue with ascending sucrose's concentrations (Berridge and Grill, 1983; Spector et al., 1998;
655 Villavicencio et al., 2018). In agreement with this definition, we found that a subpopulation LHA
656 palatability related-neurons tracked licking oromotor-related responses by increasing or decreasing
657 their activity in a sucrose-concentration dependent manner. Also, whithin a session, LHA neurons
658 tracked the sucrose's palatability rather than satiety or hunger signals. We showed that these LHA^{Vgat+}
659 neurons could function as enhancers of sucrose's palatability. Optogenetic activation of these neurons

660 can also enhance water's palatability if it is the nearest stimuli. We found an increased lick rate for
661 water during activation of these neurons as if the animal were sampling a high sucrose concentration.
662 Moreover, their activation promotes the intake of liquid sucrose (or solid granulated sugar cube). These
663 neurons also increased the consumption of other more palatable stimuli like high-fat pellets (see
664 Supplementary Figure 3; Video 2), similar to the other GABAergic neurons but in zona incerta [51]. It
665 is tempting to propose that LHA GABAergic neurons could mediate the supra-additive effects of
666 combining fats and carbohydrates such as sucrose [52], but this remains to be experimentally tested.

667

668 Although activation of LHA^{Vgat+} promotes substantial feeding behavior, it has become clear that
669 LHA^{Vgat+} neurons are not directly involved in evoking hunger [23,25,44], as AgRP neurons do [45]. In
670 agreement with these findings, we found that the intake induced by a subset of LHA^{Vgat+} convey a
671 positive valence signal that combines both stimulus proximity and palatability related information.
672 Thus, these neurons enhance the saliency of nearby hedonically positive stimuli, whether those stimuli
673 are sapid chemicals, as we show, or social cues, as in the approach behavior towards juvenile or female
674 intruders and new objects [24].

675 It is important to highlight that opto-self-activation of LHA^{Vgat+} neurons resembles many hallmark
676 behaviors evoked by LHA electrical stimulation. In particular, our results could shed some light on
677 why, at low-intensity electrical currents, lever pressing to deliver ICSs only occurs if food (or sucrose)
678 is in close proximity [6,7,53,54]. Consistent with its role in enhancing sucrose's palatability, a
679 subpopulation of GABAergic neurons could explain the long-standing puzzle of why sweet tastants
680 further potentiate the rate of LHA electrical ICSs [9]. We concluded that a subpopulation LHA^{Vgat+}
681 neurons could account for many, if not all, of these electrically induced phenomena. That said, we also
682 found differences between unspecific LHA stimulation and our targeted LHA^{Vgat+} stimulation. Unlike

electrical LHA stimulation, we found that the laser-bound feeding was observed in all tested VGAT-ChR2 mice (n = 25, Figures 4-12). In contrast, to the high variability found in rats exhibiting LHA electrically-induced feeding, one study reported that only 12 of 34 rats showed stimulus-bound feeding [55]. Similarly, a large variability was observed when unspecific bulk optogenetic stimulation activated *all* cell-types found in LHA, simultaneously [46]. These studies reported that after repeated LHA stimulation (either electrically or with optogenetics), some subjects switched from exhibiting stimulus-bound feeding to only self-stimulating, suggesting that these two processes were flexible and not correlated [37,46]. In contrast, we found that repeated stimulation of LHA^{Vgat+} neurons increases laser-induced feeding (licking). Likewise, the correlation between optogenetic self-stimulation and laser-bound feeding increases through stimulation days (Figure 8). That is, the more the animals self-stimulated, the stronger the evoked laser-bound licking was. Thus, LHA^{Vgat+} neurons are the common neural substrate for evoking both feeding and reward. Though, it was recently shown that they do it by using two projection pathways; reward via a VTA projection and feeding via the peri-Locus Coeruleus nuclei [25].

Given that LHA is involved in reward and aversion [48], we next tested whether LHA^{Vgat+} neurons could promote bitter tastants' intake. We found that opto-stimulation of LHA^{Vgat+} neurons failed to promote quinine intake, a bitter tastant, or tolerance of an aversive airpuff when sucrose was also available. Thus, these neurons play a minimal role in increasing the preference to a proximal but aversive stimulus over distal sucrose. Furthermore, in sated mice and using a single bottle test, these neurons also failed to increase quinine intake. Unexpectedly, during water deprivation, a copious quinine consumption was observed. These results agree with previous findings that chemogenetic inhibition of LHA^{Vgat+} neurons did not alter the quinine rejection responses. Thus, in sated mice, these neurons are not necessary to express hedonically negative responses induced by bitter tastants [56].

707 However, they did not explore their sufficiency. Our results showed that water deprivation temporarily
708 gated LHA^{Vgat+} neurons to promote quinine intake, and further demonstrated that their activation is
709 sufficient to increase acceptance of an aversive tastant during water deprivation.

710 The LHA comprises multiple heterogeneous and overlapping populations based on the expression of
711 genetic markers for neuropeptides, receptors, and proteins involved in the synthesis and vesicular
712 packaging of neurotransmitters [57,58]. Thus, the LHA^{Vgat+} population can be further subdivided into
713 GABA neurons expressing leptin receptor (LepRb) [58,59], or the neuropeptide galanin (Gal), or
714 neurotensin (Nts) [58,60,61]. It is known that the activation of LHA-GABA-LepRb is rewarding [62],
715 similar to LHA^{Vgat+} neurons. Likewise, LHA GABA-Gal expressing neurons are related to food reward
716 behavior, but unlike LHA^{Vgat+}, these neurons do not promote food consumption [60]. From these
717 subpopulations, only the LHA GABA-Nts neurons recapitulate some (but not all) of the behavioral
718 effects reported here. Unlike LHA^{Vgat+} neurons, a previous study found that LHA GABA-Nts neurons
719 do not increase chow intake. Instead, they promote the liquid intake of palatable tastants (water, NaCl,
720 and sucrose). In sated mice, chemogenetic activation of GABA-Nts increased the intake of bitter
721 quinine, albeit with lower magnitude, when it was the only liquid available to eat with chow food, a
722 marked contrast to our findings with broad LHA GABAergic neurons activation. Although, they did
723 not explore quinine intake, in the absence of chow food or water-deprived mice. However, they
724 performed a two-bottle test and found that GABA-Nts neurons increased water intake over quinine,
725 suggesting that these neurons cannot develop a preference to bitter tastants, similar to what we found
726 for the LHA^{Vgat+} population. Also, similar to our findings, activation of LHA GABA-Nts induced
727 water-drinking, that was further facilitated if the solution was sucrose [61]. Thus, it will be interesting
728 to determine the role that LHA GABA-Nts neurons play in encoding and potentiating sucrose's
729 palatability. It follows that the LHA contains nested functions encoded in each subpopulation (or cell-
730 types) that are then recruited selectively to exert a more refined control over feeding and reward.

731

732 A caveat of this study is that we employed bacterial artificial chromosomes (BAC) transgenic strain
733 mouse, VGAT-ChR2, that constitutively expressed ChR2 in GABAergic neurons expressing the gene
734 for the VGAT [36]. In this model, we cannot rule out unintended activation of GABAergic terminals
735 from distal regions [63], which also occurs with classic electrical stimulation. Nevertheless, in the more
736 specific transgenic model, the Vgat-ires-Cre mice has been found a similar feeding-bound behavior for
737 chow food [25], as we shown here (see Chow in Figures 9B and C; and Video 5). Moreover, the VGAT-
738 ChR2 transgenic model affords important advantages such as a consistent expression of ChR2 [64] and
739 heritable transgene expression patterns across experimental cohorts [65], which increased
740 reproducibility across animals tested. It is also a more selective model to characterize GABAergic
741 neurons (excluding the glutamatergic component) and their effects recapitulating classical effects
742 observed with electrical LHA stimulation [3,8].

743

744 In summary, here we found that at least a subpopulation of LHA^{Vgat+} neurons could be an important
745 hub that links stimulus-proximity and palatability related information to potentiate the palatability of
746 nearby energy-rich foods containing sucrose.

747

748 **Conflict of interests**

749 The authors declare no competing financial interests.

750

751 **Author Contributions**

752 A.G., A.C., J. LI., and R.G. designed research; A.G., A.C., J. LI., L.PS., and M.L. performed research;
753 M.V. contributed unpublished analytic tools; A.G., A.C., J. LI., and R.G. analyzed data; A.G. and R.G.
754 wrote the paper; all authors reviewed and approved manuscript.

755 **Funding**

756 This project was supported in part by Productos Medix 3247, Cátedra Marcos Moshinky, fundación
757 Miguel Alemán Valdés, CONACyT Grants Fronteras de la Ciencia 63 and 10862, and Problemas
758 Nacionales 464 (to R.G.).

759 **Acknowledgments**

760 Aketzali Garcia had a CONACyT doctoral fellowship, and data in this work is part of her doctoral
761 dissertation in the Posgrado en Ciencias Biomédicas of the Universidad Nacional Autónoma de
762 México. We want to thank Martin Vignovich and Professor Sidney A. Simon for helpful comments in
763 an early version of this manuscript. We thank Mario Gil Moreno for building homemade optrode, and
764 valuable help of Juan de Dios Rodriguez-Callejas during the acquisition of confocal microscope
765 images. We also thank Ricardo Gaxiola, Victor Manuel García Gómez, and Fabiola Hernandez Olvera
766 for invaluable animal care.

767

768 **References**

769 1. Anand BK, Brobeck JR. Localization of a “feeding center” in the hypothalamus of the rat.
770 Proceedings of the Society for Experimental Biology and Medicine Society for Experimental
771 Biology and Medicine. 1951;77: 323–4.

772 2. Teitelbaum P, Epstein AN. The lateral hypothalamic syndrome: recovery of feeding and
773 drinking after lateral hypothalamic lesions. Psychological review. 1962;69: 74–90.

774 3. Delgado JM, Anand BK. Increase of food intake induced by electrical stimulation of the lateral
775 hypothalamus. The American journal of physiology. 1953;172: 162–8.
776 doi:10.1152/ajplegacy.1952.172.1.162

4. Olds J, Milner P. Positive reinforcement produced by electrical stimulation of septal area and other regions of rat brain. J Comp Physiol Psychol. 1954;47: 419–427. doi:10.1037/h0058775

5. Mogenson GJ, Stevenson JA. Drinking induced by electrical stimulation of the lateral hypothalamus. Experimental neurology. 1967;17: 119–27. doi:10.1016/0014-4886(67)90139-2

6. Coons EE, Cruce JA. Lateral hypothalamus: food current intensity in maintaining self-stimulation of hunger. Science. 1968;159: 1117–9. doi:10.1126/science.159.3819.1117

7. Mendelson J. Lateral hypothalamic stimulation in satiated rats: the rewarding effects of self-induced drinking. Science. 1967;157: 1077–1079. doi:10.1126/science.157.3792.1077

8. Phillips AG, Mogenson GJ. Effects of taste on self-stimulation and induced drinking. J Comp Physiol Psychol. 1968;66: 654–660. doi:10.1037/h0026523

9. Poschel BPH. Do biological reinforcers act via the self-stimulation areas of the brain? Physiology & Behavior. 1968;3: 53–60. doi:10.1016/0031-9384(68)90031-0

10. Berthoud H-R, Münzberg H. The lateral hypothalamus as integrator of metabolic and environmental needs: from electrical self-stimulation to opto-genetics. Physiol Behav. 2011;104: 29–39. doi:10.1016/j.physbeh.2011.04.051

11. Simerly RB. Anatomical Substrates of Hypothalamic Integration. In: The Rat Nervous System. Academic Press; 2004.

12. Berk ML, Finkelstein JA. Efferent connections of the lateral hypothalamic area of the rat: an autoradiographic investigation. Brain Res Bull. 1982;8: 511–526. doi:10.1016/0361-9230(82)90009-0

13. Ter Horst GJ, Luiten PG. Phaseolus vulgaris leuco-agglutinin tracing of intrahypothalamic connections of the lateral, ventromedial, dorsomedial and paraventricular hypothalamic nuclei in the rat. Brain Res Bull. 1987;18: 191–203. doi:10.1016/0361-9230(87)90190-0

14. Ferssiwi A, Cardo B, Velley L. Gustatory preference-aversion thresholds are increased by ibotenic acid lesion of the lateral hypothalamus in the rat. Brain Res. 1987;437: 142–150. doi:10.1016/0006-8993(87)91535-6

15. Berridge KC, Valenstein ES. What psychological process mediates feeding evoked by electrical stimulation of the lateral hypothalamus? Behav Neurosci. 1991;105: 3–14. doi:10.1037//0735-7044.105.1.3

16. Schwartzbaum JS. Electrophysiology of taste, feeding and reward in lateral hypothalamus of rabbit. Physiol Behav. 1988;44: 507–526. doi:10.1016/0031-9384(88)90313-7

17. Yamamoto T, Matsuo R, Kiyomitsu Y, Kitamura R. Response properties of lateral hypothalamic neurons during ingestive behavior with special reference to licking of various taste solutions. Brain Res. 1989;481: 286–297. doi:10.1016/0006-8993(89)90805-6

811 18. Li JX, Yoshida T, Monk KJ, Katz DB. Lateral hypothalamus contains two types of palatability-
812 related taste responses with distinct dynamics. The Journal of neuroscience : the official journal
813 of the Society for Neuroscience. 2013;33: 9462–73. doi:10.1523/JNEUROSCI.3935-12.2013

814 19. Stuber GD, Wise RA. Lateral hypothalamic circuits for feeding and reward. Nature
815 neuroscience. 2016;19: 198–205. doi:10.1038/nn.4220

816 20. Gutierrez R, Fonseca E, Simon SA. The neuroscience of sugars in taste, gut-reward, feeding
817 circuits, and obesity. Cell Mol Life Sci. 2020. doi:10.1007/s00018-020-03458-2

818 21. Jennings JH, Rizzi G, Stamatakis AM, Ung RL, Stuber GD. The inhibitory circuit architecture
819 of the lateral hypothalamus orchestrates feeding. Science. 2013;341: 1517–1521.
820 doi:10.1126/science.1241812

821 22. Jennings JH, Ung RL, Resendez SL, Stamatakis AM, Taylor JG, Huang J, et al. Visualizing
822 hypothalamic network dynamics for appetitive and consummatory behaviors. Cell. 2015;160:
823 516–27. doi:10.1016/j.cell.2014.12.026

824 23. Navarro M, Olney JJ, Burnham NW, Mazzone CM, Lowery-Gionta EG, Pleil KE, et al. Lateral
825 Hypothalamus GABAergic Neurons Modulate Consummatory Behaviors Regardless of the
826 Caloric Content or Biological Relevance of the Consumed Stimuli. Neuropsychopharmacology :
827 official publication of the American College of Neuropsychopharmacology. 2016;41: 1505–12.
828 doi:10.1038/npp.2015.304

829 24. Nieh EH, Vander Weele CM, Matthews GA, Presbrey KN, Wichmann R, Leppla CA, et al.
830 Inhibitory Input from the Lateral Hypothalamus to the Ventral Tegmental Area Disinhibits
831 Dopamine Neurons and Promotes Behavioral Activation. Neuron. 2016;90: 1286–1298.
832 doi:10.1016/j.neuron.2016.04.035

833 25. Marino RAM, McDevitt RA, Gantz SC, Shen H, Pignatelli M, Xin W, et al. Control of food
834 approach and eating by a GABAergic projection from lateral hypothalamus to dorsal pons. Proc
835 Natl Acad Sci USA. 2020. doi:10.1073/pnas.1909340117

836 26. Zocchi D, Wennemuth G, Oka Y. The cellular mechanism for water detection in the mammalian
837 taste system. Nat Neurosci. 2017;20: 927–933. doi:10.1038/nn.4575

838 27. Mathis A, Mamidanna P, Cury KM, Abe T, Murthy VN, Mathis MW, et al. DeepLabCut:
839 markerless pose estimation of user-defined body parts with deep learning. Nat Neurosci.
840 2018;21: 1281–1289. doi:10.1038/s41593-018-0209-y

841 28. Nath T, Mathis A, Chen AC, Patel A, Bethge M, Mathis MW. Using DeepLabCut for 3D
842 markerless pose estimation across species and behaviors. Nat Protoc. 2019;14: 2152–2176.
843 doi:10.1038/s41596-019-0176-0

844 29. Villavicencio M, Moreno MG, Simon SA, Gutierrez R. Encoding of Sucrose's Palatability in
845 the Nucleus Accumbens Shell and Its Modulation by Exteroceptive Auditory Cues. Front
846 Neurosci. 2018;12: 265. doi:10.3389/fnins.2018.00265

847 30. Berridge KC, Grill HJ. Alternating ingestive and aversive consummatory responses suggest a
848 two-dimensional analysis of palatability in rats. Behavioral neuroscience. 1983;97: 563–73.

849 31. Spector AC, Klumpp PA, Kaplan JM. Analytical issues in the evaluation of food deprivation
850 and sucrose concentration effects on the microstructure of licking behavior in the rat.
851 Behavioral neuroscience. 1998;112: 678–94.

852 32. Gutierrez R, Simon SA, Nicolelis MA. Licking-induced synchrony in the taste-reward circuit
853 improves cue discrimination during learning. The Journal of neuroscience : the official journal
854 of the Society for Neuroscience. 2010;30: 287–303. doi:10.1523/JNEUROSCI.0855-09.2010

855 33. Gutierrez R, Carmena JM, Nicolelis MAL, Simon SA. Orbitofrontal ensemble activity monitors
856 licking and distinguishes among natural rewards. J Neurophysiol. 2006;95: 119–133.
857 doi:10.1152/jn.00467.2005

858 34. Buonomano DV. Timing of neural responses in cortical organotypic slices. Proc Natl Acad Sci
859 USA. 2003;100: 4897–4902. doi:10.1073/pnas.0736909100

860 35. Glendinning JI, Chyou S, Lin I, Onishi M, Patel P, Zheng KH. Initial licking responses of mice
861 to sweeteners: effects of tas1r3 polymorphisms. Chem Senses. 2005;30: 601–614.
862 doi:10.1093/chemse/bji054

863 36. Zhao S, Ting JT, Atallah HE, Qiu L, Tan J, Gloss B, et al. Cell type-specific channelrhodopsin-
864 2 transgenic mice for optogenetic dissection of neural circuitry function. Nature methods.
865 2011;8: 745–52.

866 37. Gigante ED, Benaliouad F, Zamora-Olivencia V, Wise RA. Optogenetic Activation of a Lateral
867 Hypothalamic-Ventral Tegmental Drive-Reward Pathway. PLoS ONE. 2016;11: e0158885.
868 doi:10.1371/journal.pone.0158885

869 38. Norgren R. Gustatory responses in the hypothalamus. Brain Res. 1970;21: 63–77.
870 doi:10.1016/0006-8993(70)90021-1

871 39. Schwartzbaum JS. Electrophysiology of taste, feeding and reward in lateral hypothalamus of
872 rabbit. Physiol Behav. 1988;44: 507–526. doi:10.1016/0031-9384(88)90313-7

873 40. Grill, Berridge KC. Taste reactivity as a measure of the neural control of palatability. Progress
874 in Psychobiology and Physiological Psychology. Orlando, FL.: Academic Press; 1985. pp. 1–
875 54.

876 41. Sclafani A. The Hedonics of Sugar and Starch. The hedonics of taste. New York, NY.:
877 Lawrence Erlbaum Associates, Inc; 1991. pp. 59–87.

878 42. O'Connor EC, Kremer Y, Lefort S, Harada M, Pascoli V, Rohner C, et al. Accumbal D1R
879 Neurons Projecting to Lateral Hypothalamus Authorize Feeding. Neuron. 2015;88: 553–564.
880 doi:10.1016/j.neuron.2015.09.038

881 43. Nieh EH, Matthews GA, Allsop SA, Presbrey KN, Leppla CA, Wichmann R, et al. Decoding
882 neural circuits that control compulsive sucrose seeking. Cell. 2015;160: 528–541.
883 doi:10.1016/j.cell.2015.01.003

884 44. Burnett CJ, Li C, Webber E, Tsaousidou E, Xue SY, Brüning JC, et al. Hunger-Driven
885 Motivational State Competition. Neuron. 2016;92: 187–201. doi:10.1016/j.neuron.2016.08.032

886 45. Chen Y, Lin Y-C, Zimmerman CA, Essner RA, Knight ZA. Hunger neurons drive feeding
887 through a sustained, positive reinforcement signal. Elife. 2016;5. doi:10.7554/eLife.18640

888 46. Urstadt KR, Berridge KC. Optogenetic mapping of feeding and self-stimulation within the
889 lateral hypothalamus of the rat. PLoS ONE. 2020;15: e0224301.
890 doi:10.1371/journal.pone.0224301

891 47. Sharpe MJ, Marchant NJ, Whitaker LR, Richie CT, Zhang YJ, Campbell EJ, et al. Lateral
892 Hypothalamic GABAergic Neurons Encode Reward Predictions that Are Relayed to the Ventral
893 Tegmental Area to Regulate Learning. Current Biology. 2017;27: 2089-2100.e5.
894 doi:10.1016/j.cub.2017.06.024

895 48. Ono T, Nakamura K, Nishijo H, Fukuda M. Hypothalamic neuron involvement in integration of
896 reward, aversion, and cue signals. J Neurophysiol. 1986;56: 63–79. doi:10.1152/jn.1986.56.1.63

897 49. Rolls ET. Taste, olfactory, and food reward value processing in the brain. Prog Neurobiol.
898 2015;127–128: 64–90. doi:10.1016/j.pneurobio.2015.03.002

899 50. Karádi Z, Oomura Y, Nishino H, Scott TR, Lénárd L, Aou S. Responses of lateral hypothalamic
900 glucose-sensitive and glucose-insensitive neurons to chemical stimuli in behaving rhesus
901 monkeys. J Neurophysiol. 1992;67: 389–400. doi:10.1152/jn.1992.67.2.389

902 51. Zhang X, van den Pol AN. Rapid binge-like eating and body weight gain driven by zona incerta
903 GABA neuron activation. Science. 2017;356: 853–859. doi:10.1126/science.aam7100

904 52. DiFeliceantonio AG, Coppin G, Rigoux L, Edwin Thanarajah S, Dagher A, Tittgemeyer M, et
905 al. Supra-Additive Effects of Combining Fat and Carbohydrate on Food Reward. Cell Metab.
906 2018;28: 33-44.e3. doi:10.1016/j.cmet.2018.05.018

907 53. Valenstein ES, Cox VC, Kakolewski JW. Modification of Motivated Behavior Elicited by
908 Electrical Stimulation of the Hypothalamus. Science. 1968;159: 1119–1121.
909 doi:10.1126/science.159.3819.1119

910 54. Valenstein ES, Phillips AG. Stimulus-bound eating and deprivation from prior contact with
911 food pellets. Physiology & Behavior. 1970;5: 279–282. doi:10.1016/0031-9384(70)90099-5

912 55. Valenstein ES, Cox VC. Influence of hunger, thirst, and previous experience in the test chamber
913 on stimulus-bound eating and drinking. J Comp Physiol Psychol. 1970;70: 189–199.
914 doi:10.1037/h0028708

915 56. Fu O, Iwai Y, Narukawa M, Ishikawa AW, Ishii KK, Murata K, et al. Hypothalamic neuronal
916 circuits regulating hunger-induced taste modification. Nat Commun. 2019;10: 1–14.
917 doi:10.1038/s41467-019-12478-x

918 57. Bonnavion P, Mickelsen LE, Fujita A, de Lecea L, Jackson AC. Hubs and spokes of the lateral
919 hypothalamus: cell types, circuits and behaviour. J Physiol (Lond). 2016;594: 6443–6462.
920 doi:10.1113/JP271946

921 58. Mickelsen LE, Bolisetty M, Chimileski BR, Fujita A, Beltrami EJ, Costanzo JT, et al. Single-
922 cell transcriptomic analysis of the lateral hypothalamic area reveals molecularly distinct

923 populations of inhibitory and excitatory neurons. Nat Neurosci. 2019;22: 642–656.
924 doi:10.1038/s41593-019-0349-8

925 59. Leinninger GM, Jo Y-H, Leshan RL, Louis GW, Yang H, Barrera JG, et al. Leptin acts via
926 leptin receptor-expressing lateral hypothalamic neurons to modulate the mesolimbic dopamine
927 system and suppress feeding. Cell Metab. 2009;10: 89–98. doi:10.1016/j.cmet.2009.06.011

928 60. Qualls-Creekmore E, Yu S, Francois M, Hoang J, Huesing C, Bruce-Keller A, et al. Galanin-
929 Expressing GABA Neurons in the Lateral Hypothalamus Modulate Food Reward and
930 Noncompulsive Locomotion. J Neurosci. 2017;37: 6053–6065. doi:10.1523/JNEUROSCI.0155-
931 17.2017

932 61. Kurt G, Woodworth HL, Fowler S, Bugescu R, Leinninger GM. Activation of lateral
933 hypothalamic area neurotensin-expressing neurons promotes drinking. Neuropharmacology.
934 2019;154: 13–21. doi:10.1016/j.neuropharm.2018.09.038

935 62. Giardino WJ, Eban-Rothschild A, Christoffel DJ, Li S-B, Malenka RC, de Lecea L. Parallel
936 circuits from the bed nuclei of stria terminalis to the lateral hypothalamus drive opposing
937 emotional states. Nat Neurosci. 2018;21: 1084–1095. doi:10.1038/s41593-018-0198-x

938 63. Thoeni S, Loureiro M, O'Connor EC, Lüscher C. Depression of Accumbal to Lateral
939 Hypothalamic Synapses Gates Overeating. Neuron. 2020. doi:10.1016/j.neuron.2020.03.029

940 64. Zeng H, Madisen L. Mouse transgenic approaches in optogenetics. Prog Brain Res. 2012;196:
941 193–213. doi:10.1016/B978-0-444-59426-6.00010-0

942 65. Ting JT, Feng G. Development of transgenic animals for optogenetic manipulation of
943 mammalian nervous system function: progress and prospects for behavioral neuroscience.
944 Behav Brain Res. 2013;255: 3–18. doi:10.1016/j.bbr.2013.02.037

945
946
947
948
949
950
951
952
953
954
955
956
957
958
959
960
961
962
963
964

Figures

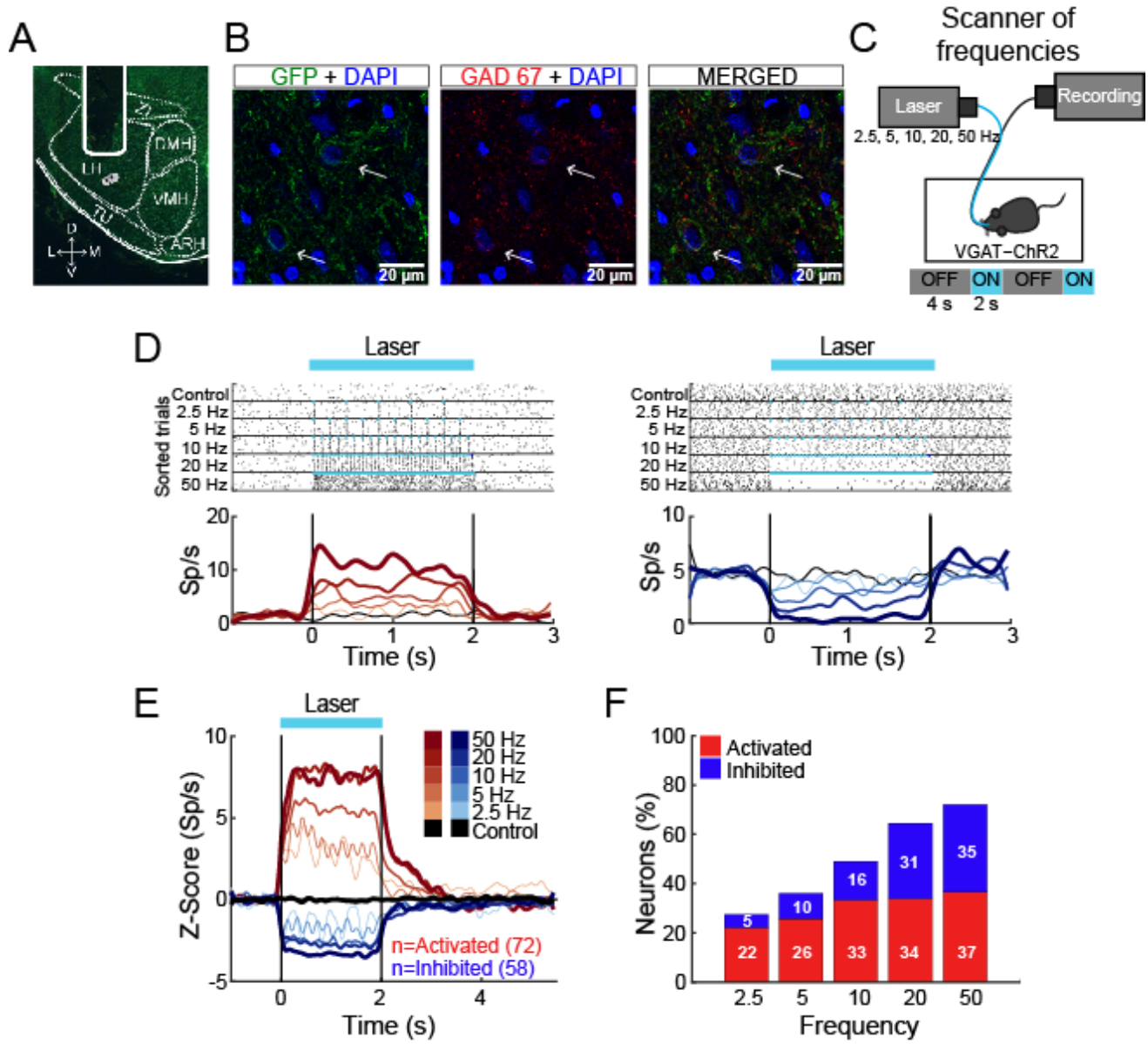

Figure 1. The 50 Hz stimulation evoked the largest LHA neuronal responses. **(A)** Representative location of an optrode in LHA of VGAT-ChR2 mice. **(B)** Confocal images from LHA immunostained for GFP (green), GAD67 (red), and DAPI (blue). Arrows indicate the colocalization of ChR2-EYFP and GAD67 (see merged). **(C)** Schematic of optrode recordings in LHA during control trials (with no-laser) and opto-stimulation at 2.5, 5, 10, 20, and 50 Hz delivered randomly. In each trial, the laser had a cycle of 2 s on and 4 s off. **(D)** Representative raster plots of two neurons recorded in LHA, the first one was activated (left panel), and the second inhibited (right panel) during opto-stimulation. Spiking responses were aligned (Time = 0 s) to the first laser pulse. Black ticks depict action potentials and

982 blue marks laser pulses. For visualization purposes, it is only shown laser pulses in the first trial for
983 each trial type. Below are the corresponding PSTHs (firing rates, Sp/s). Red and blue ascending
984 gradients indicate the frequency of stimulation (see E for the color bar). Black trace represents activity
985 during control trials without laser. Vertical black lines indicate laser onset (Time = 0 s) and offset
986 (Time = 2 s), respectively. **(E)** Normalized Z-score population responses of LHA neurons recorded
987 from n = 5 VGAT-ChR2 mice. Red and blue colors depict activated or inhibited responses,
988 respectively, relative to baseline (-1 to 0 s), thickness, and gradient colors indicate higher stimulation
989 frequencies. Black trace illustrates neural activity during control trials for all recorded neurons (n =
990 186). **(F)** Percentage of neurons recruited as a function of stimulation frequency.

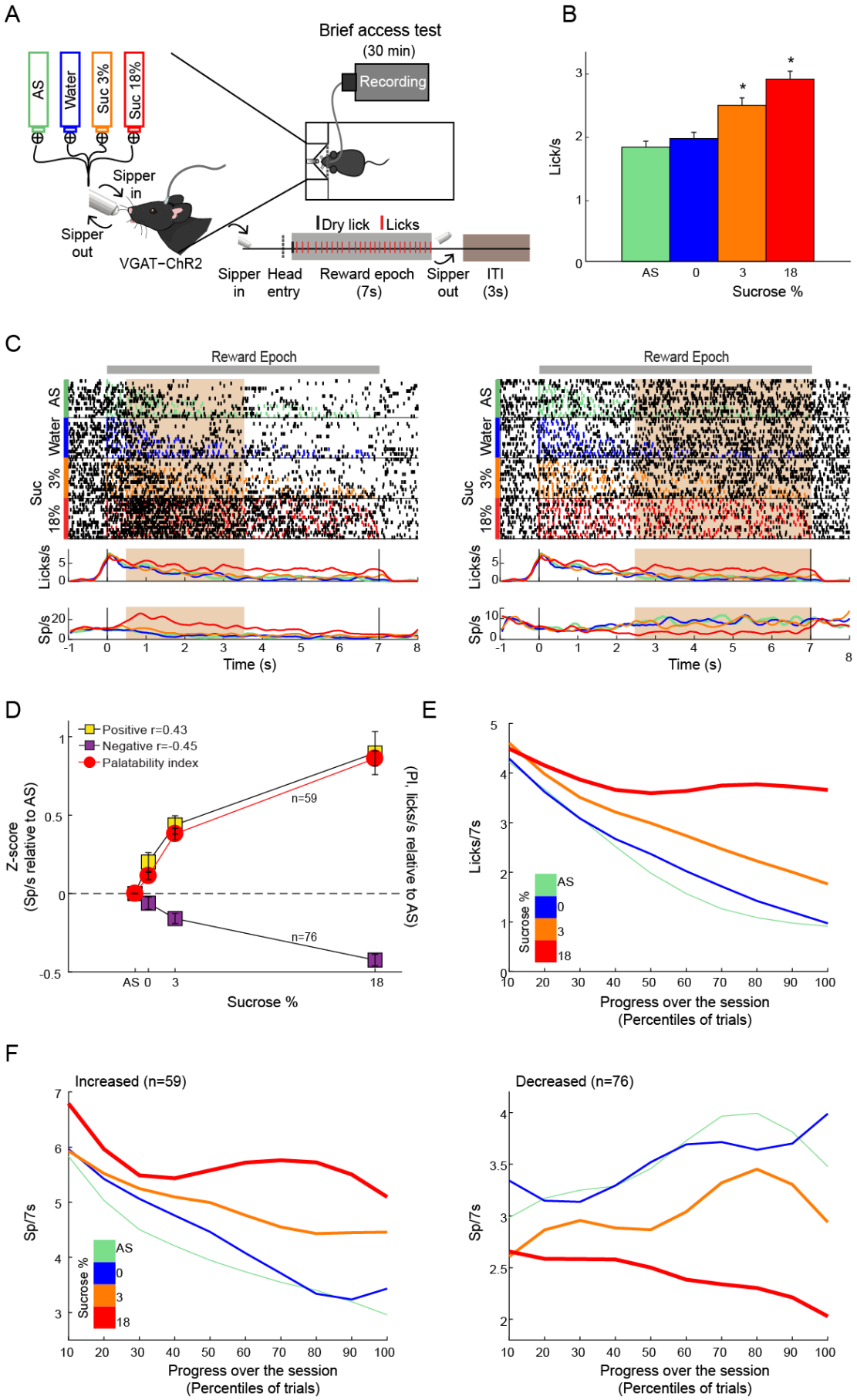
A
Brief access test
(30 min)
Recording
AS
Water
Suc 3%
Suc 18%
Sipper in
Sipper out
VGAT−ChR2
Dry lick
Licks
Sipper in
Head entry
Reward epoch (7s)
Sipper out
ITI (3s)
B
Lick/s
Sucrose %
C
Reward Epoch
Suc
Licks/s
Sp/s
Time (s)
D
Positive r=0.43
Negative r=-0.45
Palatability index
Z-score (Sp/s relative to AS)
(PI, licks/s relative to AS)
n=59
n=76
Sucrose %
E
Licks/7s
Progress over the session (Percentiles of trials)
F
Increased (n=59)
Decreased (n=76)
Sp/7s
Progress over the session (Percentiles of trials)

991

Figure 2. LHA neurons process palatability-related information. **(A)** Brief access taste and optotagging setup depicting a behavioral box equipped with a computer-controlled retractile sipper that for each lick independently delivers a drop of artificial saliva (AS), water, sucrose 3%, or 18% concentrations. After a head entry (dashed line), the first dry lick (black line) enables the 7 s reward epoch. During this period, in each lick (red), a drop of the four tastants was randomly delivered. After the reward epoch, the sipper was retracted for an Intertrial Interval (ITI) of 3 s and then re-extended to start a new trial. **(B)** Average lick rate during the entire reward epoch, reflecting greater palatability as a function of sucrose concentration. **(C)** Representative raster plot of two LHA neurons recorded while mice performed a brief access test. Spikes are plotted as black ticks, whereas licks for each tastant are in color-coded (green, AS; blue, water; orange, sucrose 3%; red, sucrose 18%). Below are corresponding peristimulus time histograms (PSTHs) of lick rate (Licks /s) and firing rate (Spikes/s; Sp/s) as a function of trial type. Neuronal responses were aligned (Time = 0 s) to the first rewarded lick. The brown rectangles depict the "best" window with the maximum Pearson correlation coefficient between firing rates and sucrose's palatability index (PI). The left and right raster plots displayed two neurons with a positive and negative correlation, respectively. **(D)** Z-score normalized activity (relative to AS trials) for LHA neurons with either positive or negative correlation against PI (red circles). **(E)** Population PSTHs of the lick rates given in the Reward epoch (Licks/7s) as a function of trial type, divided into blocks of 10th percentiles of trials each. **(F)** Population PSTHs of the firing rate during the Reward epoch (spikes/ 7s) of the palatability-related neurons across the session for each trial type. *Left panel* depicts neurons that fired more to higher sucrose concentrations (positive sucrose's palatability correlation; (D) yellow), whereas, *right panel* illustrates neurons with decreasing firing rates as the sucrose concentration increased (i.e., negative correlation with sucrose's palatability; (D) purple).

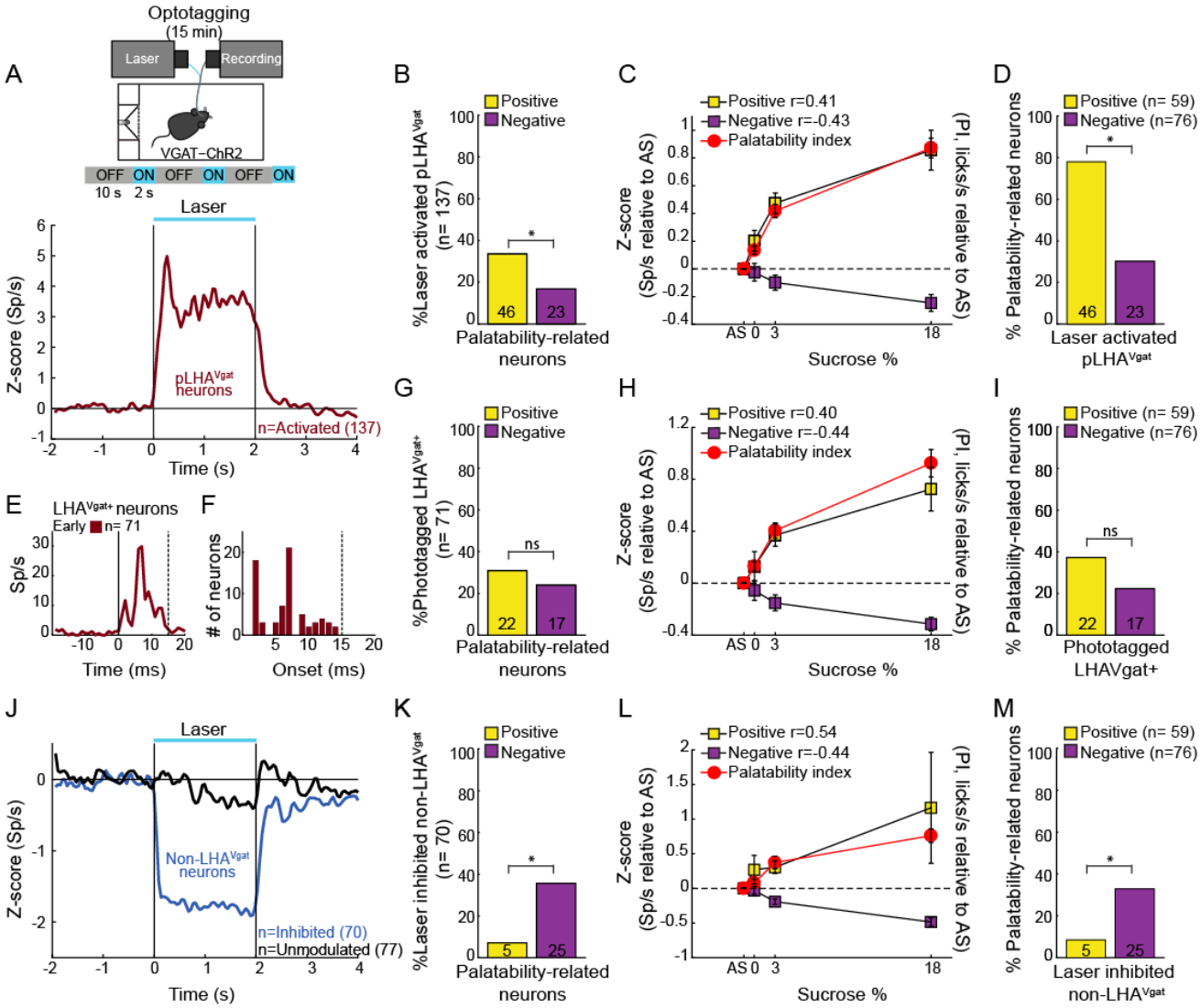

Figure 3. A subpopulation of LHA^{Vgat+} neurons encodes sucrose's palatability. **(A)** To confirm the LHA^{Vgat+} neurons' identity after the brief access test, we performed laser opto-stimulation in a cycle 2 s on (at 50 Hz) and 10 s off over 15 min session. In this phase, mice had no access to the sipper (*above panel*), *below* the normalized Z-score population activity of all 284 LHA neurons recorded from 3 VGAT-ChR2 mice. Responses were aligned to the laser onset (Time = 0 s), relative to baseline (-1 to 0 s) activity. The red line depicts the responses of activated putative pLHA^{Vgat} neurons. **(B)** Percentage of laser-activated pLHA^{Vgat+} neurons whose activity (in the brief access test) also positively or negatively correlates with sucrose's PI. * $p < 0.01$, chi-square. **(C)** Z-score activity (relative to AS) for all activated pLHA^{Vgat} neurons and its correlation with the sucrose's PI. **(D)** Percentage of Positive or Negative laser-activated palatability-related neurons. * $p < 0.0001$, chi-square. **(E)** PSTH of identified (opto-tagged) LHA^{Vgat+} neurons exhibiting early evoked responses (i.e., ChR2 expressing cells). **(F)** Histogram of opto-tagged LHA^{Vgat+} neurons with evoked early responses (latencies < 15 ms) from laser onset. **(G-I)** same conventions as in B-D, but for opto-tagged LHA^{Vgat+} neurons encoding sucrose's palatability. **(J-M)** Non-LHA^{Vgat} neurons that negatively encode sucrose's palatability. ***J,*** Blue and black traces correspond to Inhibited (Non-LHA^{Vgat+} neurons) and Unmodulated responses, respectively. Same conventions as in (*A*). **(K-M)** same conventions as in B-D, * $p < 0.001$, chi-square.

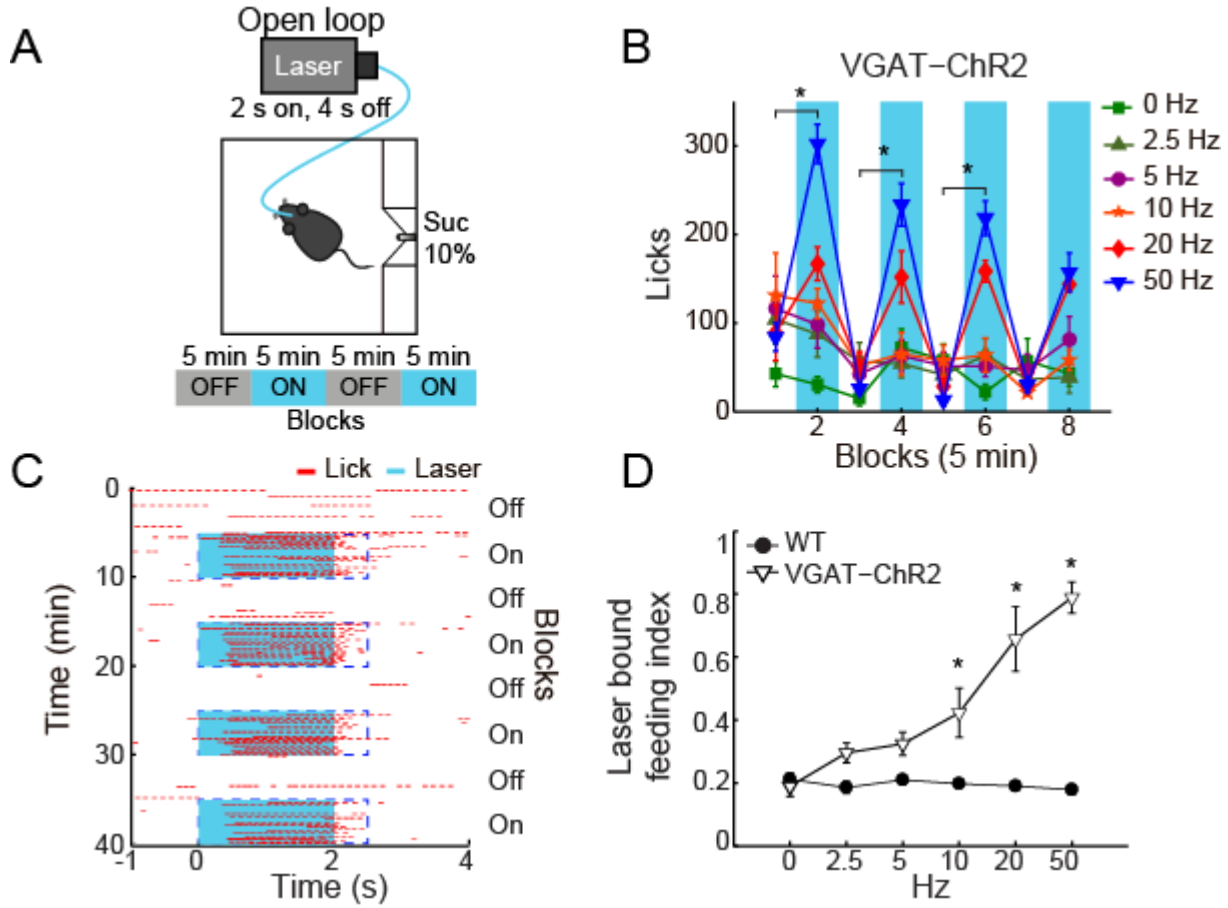

Figure 4. In sated VGAT-ChR2 mice, 50 Hz stimulation of LHA^{Vgat+} neurons induced the greatest intake of sucrose. ***A,*** Behavioral setup for open-loop stimulation, where the laser was turned on regardless of the mice's behavior. The box was equipped with a central sipper where mice had free access to 10 % sucrose. Open-loop stimulation comprised 5 min block without laser followed by opto-stimulation for 5 min, in a cycle 2 s on – 4 s off, during a 40 min session. VGAT-ChR2 (n = 3) and WT (n = 5) mice received stimulation of only one of the following frequencies in ascending order per session 0, 2.5, 5, 10, 20, and 50 Hz. ***B,*** Opto-stimulation of LHA^{Vgat+} neurons induced sucrose (10%) intake in a frequency-dependent manner that peaked at 50 Hz. * Denotes statistically significant difference ($p < 0.001$) between no-laser and laser stimulated blocks at 50 Hz. Besides mice were sated, the lower intake at 0 Hz could be due to the lack of experience drinking in the novel box. ***C,*** Representative raster plot of open-loop stimulation from a VGAT-ChR2 mouse at 50 Hz. Lick responses (red ticks) were aligned to laser onset (blue rectangles, opto-stimulation period). The laser bound index was the number of licks within 2.5 s from laser onset (dashed blue rectangles) divided by total licks. ***D,*** The laser bound feeding index of VGAT-ChR2 increased as a function of the laser frequency. * Indicates significant difference from WT mice ($p < 0.01$), using a Two-way ANOVA followed by the Holm Sidak test. In this and other figures, data represent mean ± SEM.

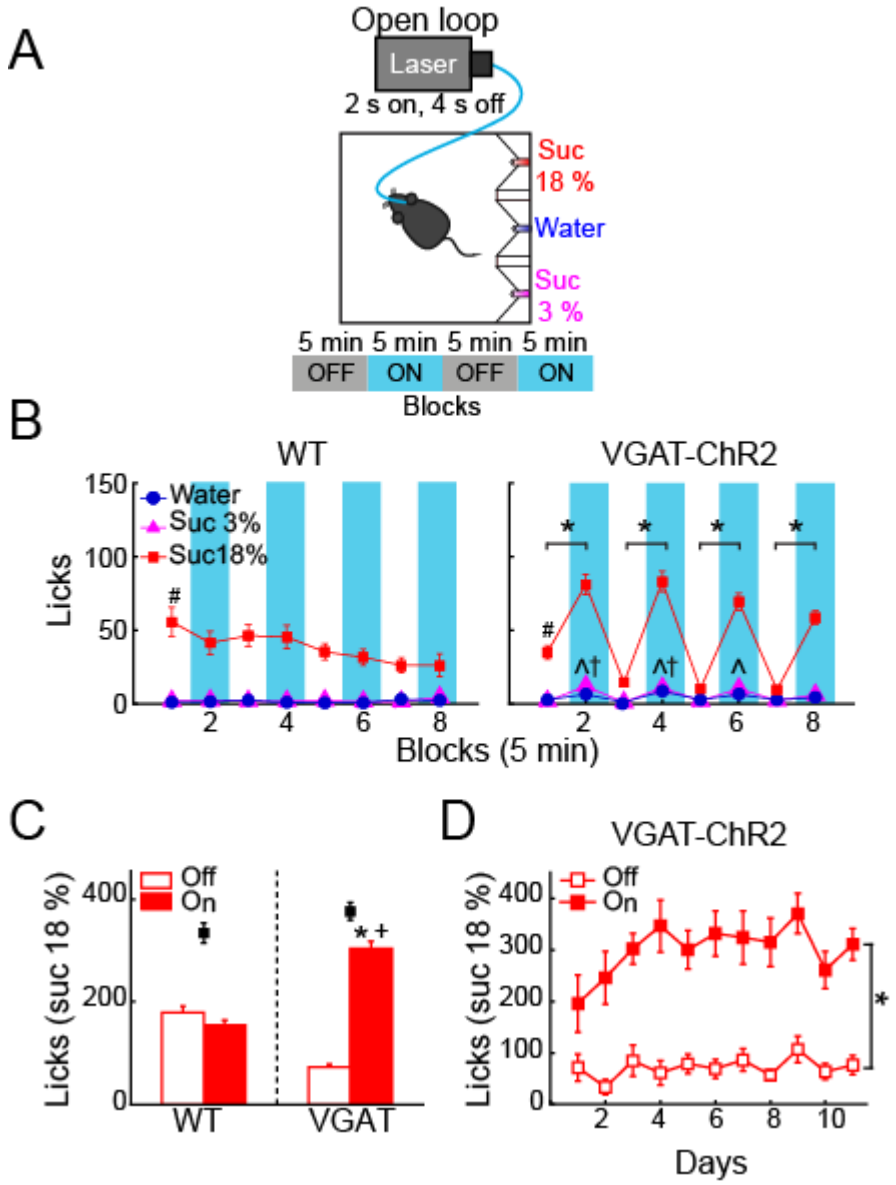

1048

1049 **Figure 5.** Open loop stimulation of LHA^{Vgat+} neurons biases consumption towards the most palatable
1050 tastant and reinforce intake during opto-stimulation. **(A)** Behavioral protocol. Sated mice (n = 6 WT
1051 and n = 12 VGAT-ChR2) were located in an operant box equipped with three ports. The left port
1052 contained sucrose 18%, the central port water, and the right port sucrose 3%, counterbalanced across
1053 individuals. For details of open loop, see Figure 4A. **(B)** *Left and right panel*, number of licks for each
1054 gustatory stimulus for WT and VGAT-ChR2 mice. Note that the VGAT-ChR2 mice increased
1055 consumption of the most palatable stimuli available (sucrose 18%) mainly in opto-stimulated blocks
1056 (blue rectangles), while it decreased intake in blocks without laser. **(C)** Mean licks for sucrose 18%,
1057 during blocks with laser on and off from WT and VGAT-ChR2 mice. Black squares show the total
1058 licks given for each group. **(D)** Licks for sucrose 18% during blocks with or without laser across days.
1059 * Indicates a significant difference ($p < 0.0001$) between laser and no-laser blocks. # $p < 0.0001$
1060 statistically significant difference between sucrose 18% and the other stimuli. ^ $p < 0.01$ between WT
1061 and VGAT-ChR2 for sucrose 3%; † $p < 0.01$ higher intake of water of VGAT-ChR2 compared with
1062 WT;+ $p < 0.0001$ higher consumption of VGAT-ChR2 compared with WT for sucrose 18% during
1063 blocks with laser. Using a two-way ANOVA and RM ANOVA followed by the Holm Sidak test.

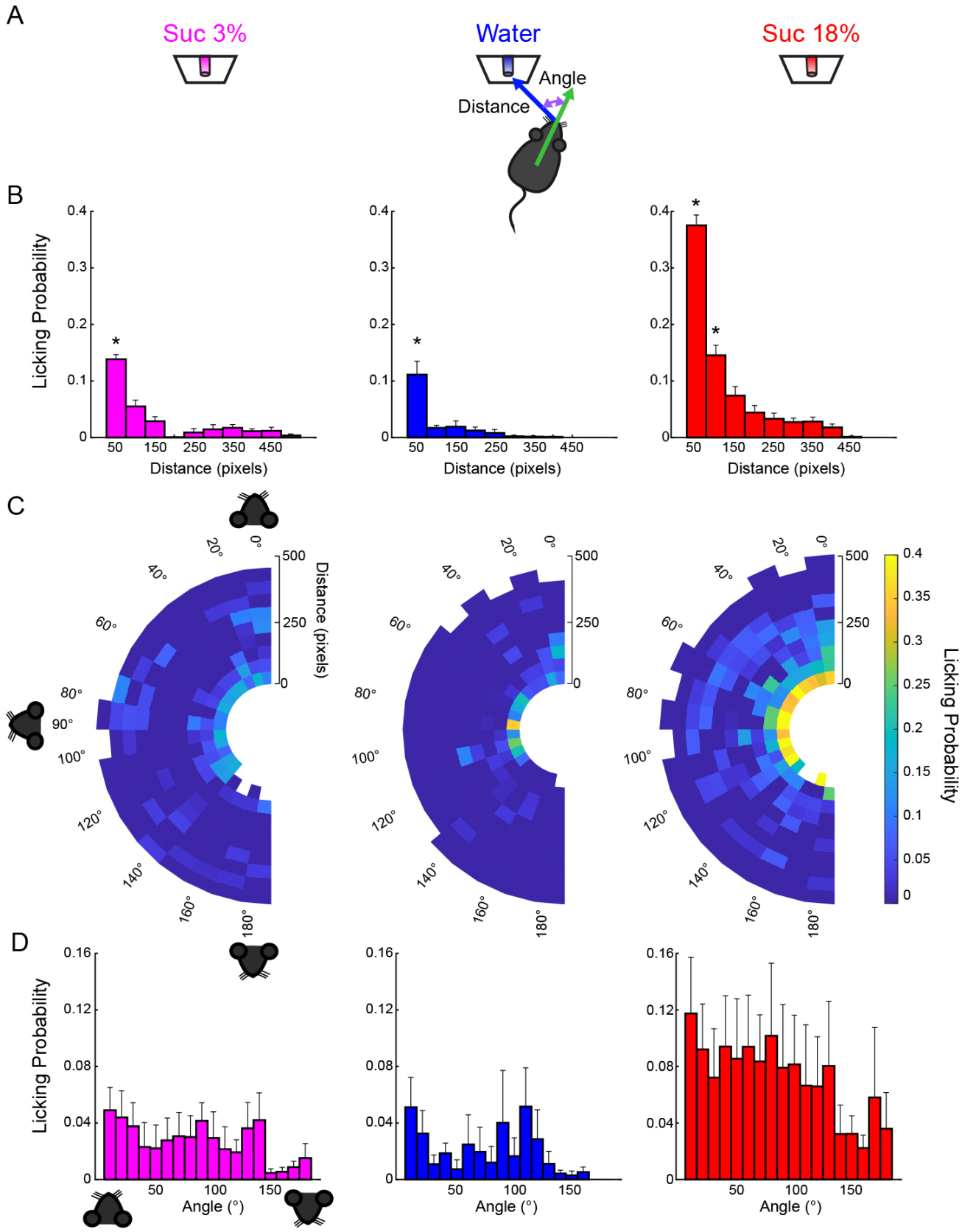

Figure 6. Licking probability increased as a function of distance. **(A)** Schematics for video tracking (see Materials and Methods). We calculated the distance and the head angle between the mouse's nose and each of the three sippers containing sucrose 3%, water, or sucrose 18% for each laser onset. **(B*)*** It

depicts the probability that laser onset evoked licking as a function of the mouse's distance relative to each sipper. **(C)** Polar plots depict the licking probability after laser onset, given distance and angle of the mouse relative to a licking sipper. At the onset of each laser stimulation, we computed the head angle and distance relative to each sipper, and, in the following 6 s window, we tally if the mouse licked to any sipper. We normalized by dividing the number of times licking was elicited by the number of first lasers occurring on those coordinates. The drawing of the mice's head illustrates that if a mouse was facing towards the sipper, the angle is 0°, in a perpendicular position (90°), or 180° if it was looking at the opposite direction. **(D)** The probability of licking after laser stimulation versus the angle between head direction and the sipper. * Indicates significantly different ($p < 0.001$) from all other distances. One-way ANOVA followed by the Holm Sidak test.

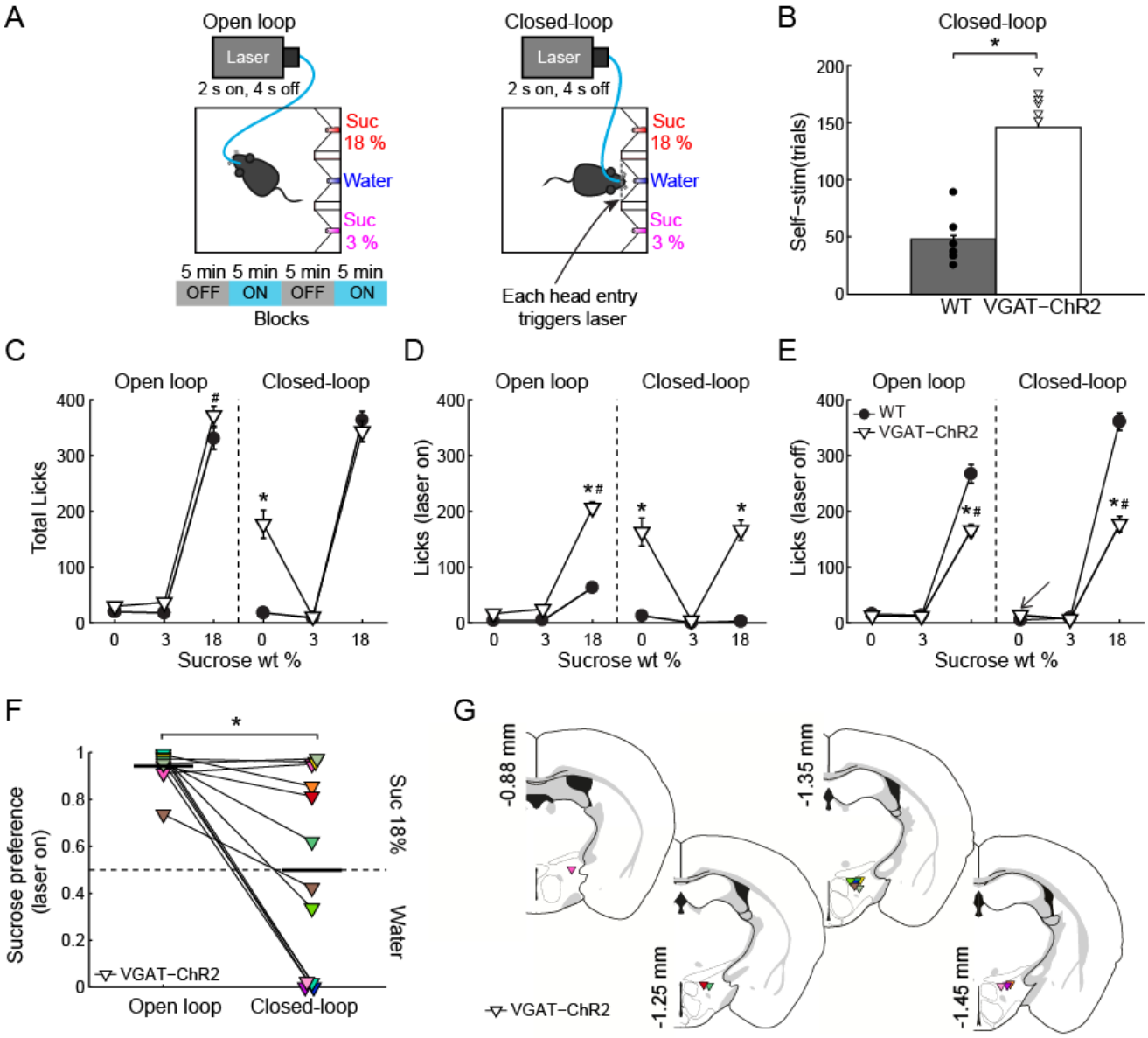

Figure 7. If stimulation occurred near the less palatable stimulus, LHA^{Vgat+} neurons induced water intake despite sucrose. **(A)** For the open loop stimulation, the laser was activated (2s on, 4s off) regardless of behavior and mice position. Same mice and conventions as in Figure 5*A*. In the closed-

loop configuration, the laser was triggered by a head entry in the central port. **(B)** The number of laser activations during the closed-loop protocol. The VGAT-ChR2 mice self-stimulate more than the WT mice. Each dot and triangle represent a single mouse. Unpaired t-test. **(C)** The total number of licks for each stimulus given during the entire session. In the open loop both mice groups licked more sucrose 18% than water or sucrose 3%. However, in the closed-loop configuration, the VGAT-ChR2 consumed more water (0 % sucrose) than the WT mice. **(D)** The number of licks evoked during 2.5 s after laser onset for each gustatory stimulus. **(E)** The number of licks when laser was turned off for each gustatory stimulus. **(F)** The water-sucrose 18% preference index from VGAT-ChR2 mice during photostimulation was defined as the number of licks of 18% sucrose divided by total licks for sucrose 18% + water. Thus, values higher than 0.5 indicate sucrose 18%, and values lower than 0.5 prefer water. Some VGAT-ChR2 mice preferred water over sucrose. The horizontal black lines indicate mean preference in both stimulation protocols. Paired t-test. **(G)** Fiber optic location in the LHA of VGAT-ChR2 mice. * $p < 0.0001$ Indicates significant difference from WT mice and stimulation protocols. # $p < 0.0001$ between sucrose 18% and the other stimuli. Two-way ANOVA followed by the Holm Sidak test.

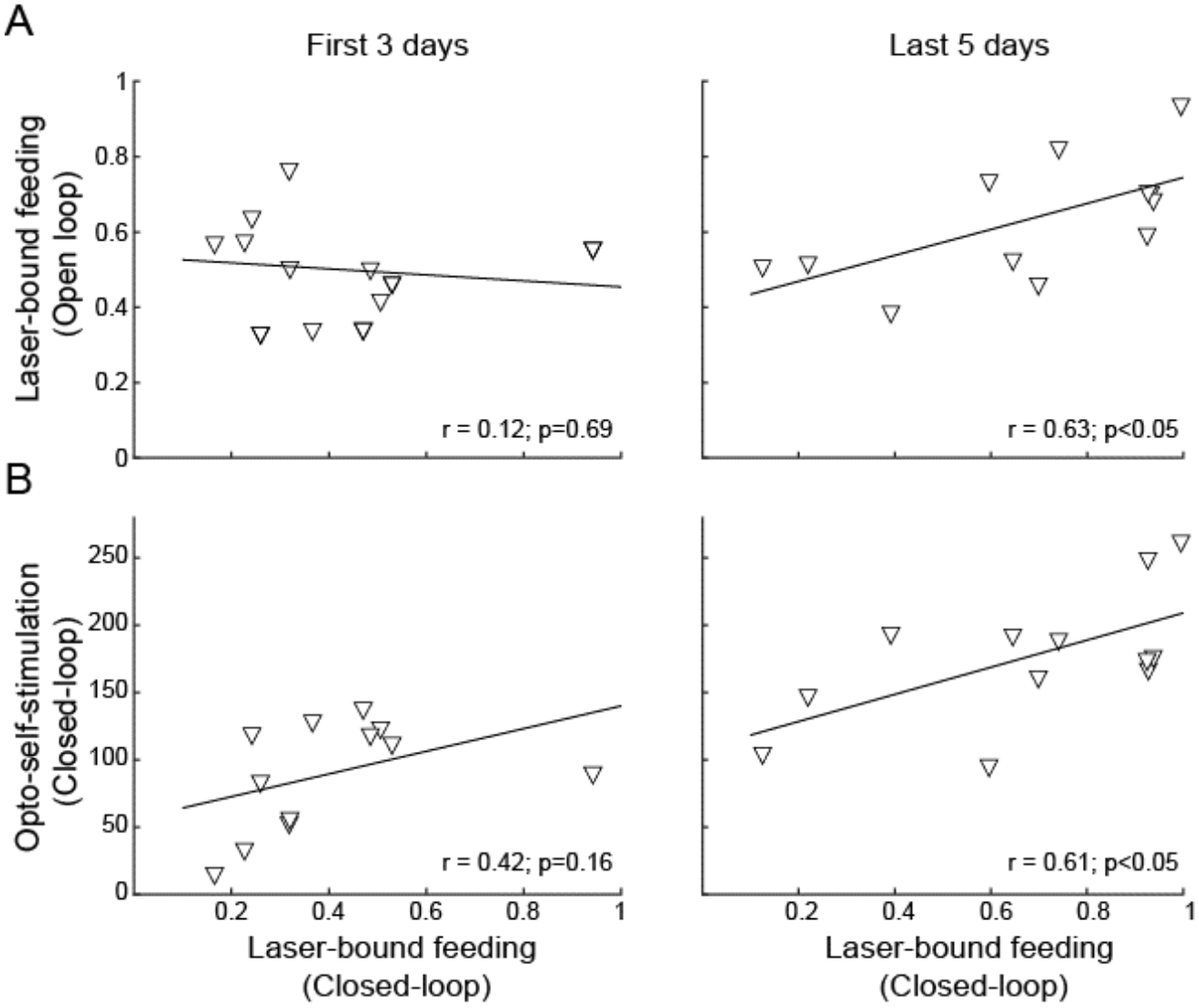

Figure 8. After repeated activation of LHA^{Vgat+} neurons, laser-bound feeding (in open vs. closed-loop) strengthened and exhibited a positive correlation. **(A)** Scatter plots showing the relationship between

laser-bound feeding (licks given during the 2.5 s window from laser onset relative to total licks in the session) in both open loop and closed-loop tasks during the first 3 days (l*eft panel*) and the last 5 days of opto-stimulation of open loop vs. opto-self-stimulation of the closed-loop protocols (*right panel*). **(B)** Likewise, after repeated activation, both opto-self-stimulations and laser-bound feeding (licking) showed a significant correlation. Scatter depicting the average number of opto-self-stimulations vs. the laser-bound feeding observed in the closed-loop protocol.

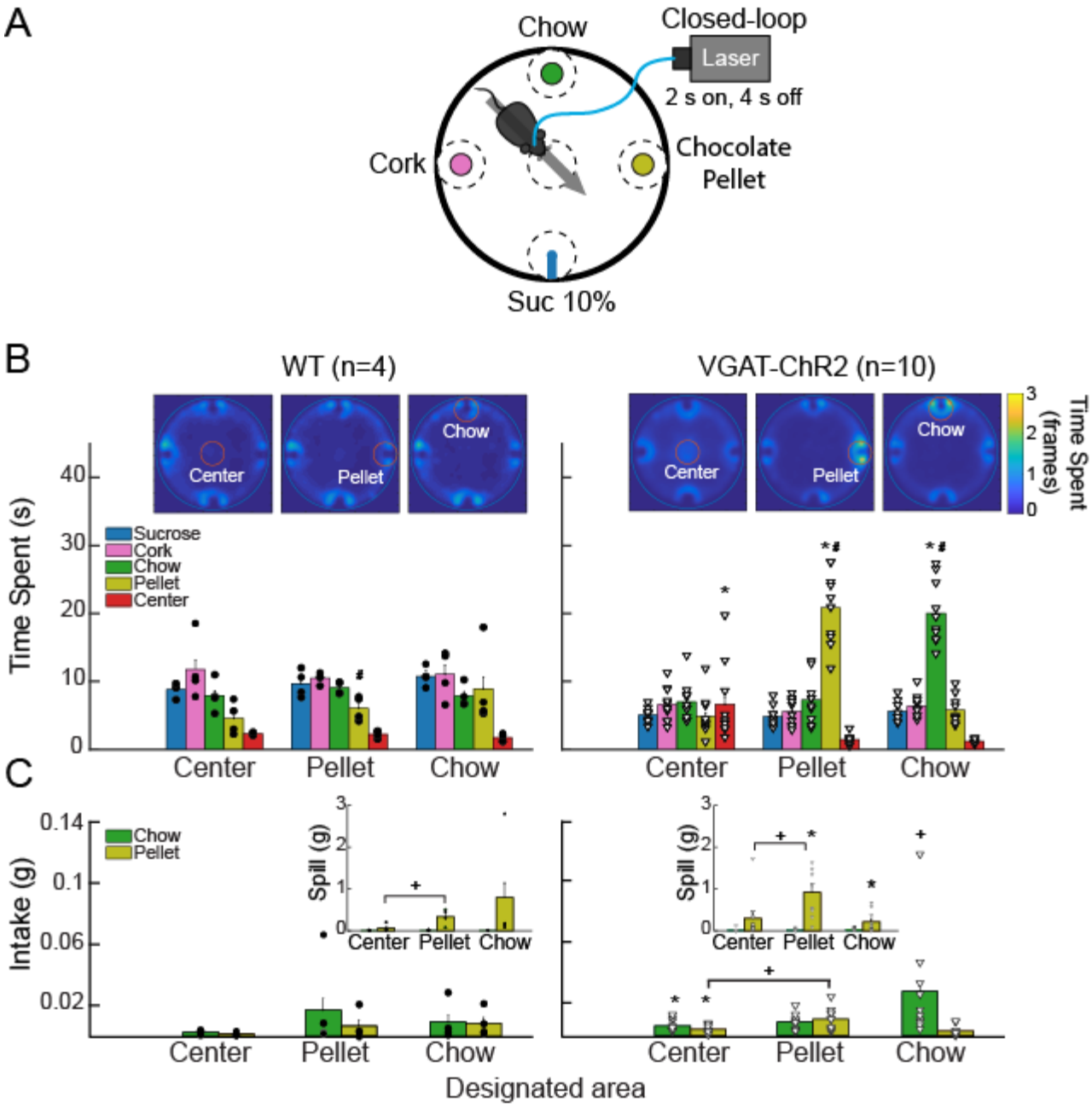

Figure 9. Stimulation of LHA^{Vgat+} neurons is rewarding and biases approach towards the nearest stimulus. **(A)** Different stimuli (plates containing cork, Chow, chocolate pellets, or a sipper filled with 10% liquid sucrose) were presented simultaneously in a circular arena. In this task, when mice cross a designated area (dashed circles), the laser was turned on (2 s on; 4 s off) in a 40 min session. Thus, a mouse had to leave and re-enter the designated area to receive a new opto-self-stimulation. Only one designated area was used per session, and it remained in the same position for up to 3 or 4 consecutive

days. **(B)** Heat map and time spent from a representative WT (left panel) and VGAT-ChR2 mice (right panels), when the designated area was either the center, the pellet, or the Chow (see red circles for the currently designated zone). Colorbar indicates the number of frames the subject was detected in a given pixel; higher values indicate it remained in the same place for a longer time. *Below*, bar graphs depict the time spent in seconds exploring the designated area (within a radius of 5 cm). Each dot and triangle represent a single individual. Though mice normally avoid exploring the center of an open field, opto-self-stimulation in the center zone increased the time transgenic mice spent exploring it, compared with WT. Transgenic mice spent more time exploring the chocolate pellets and the Chow food when they were the designated zones. **(C)** Intake of chocolate pellet and Chow. Activation of LHA^{Vgat+} neurons in the center zone increased the consumption of chocolate pellets and chow compared with WT. *Inset*: Spill from chocolate pellets and chow. * Indicates statistically significant difference ($p < 0.05$) from WT. + $p < 0.05$ shows a significant increase in consumption and spill during the session that a designated area was opto-self-stimulated relative to the sessions where the center was opto-self-stimulated. Unpaired Student *t*-test. # $p < 0.01$ indicates significant difference between designated area opto-stimulated and the other open field areas. One-way ANOVA followed by the Holm Sidak test. See Video 5.

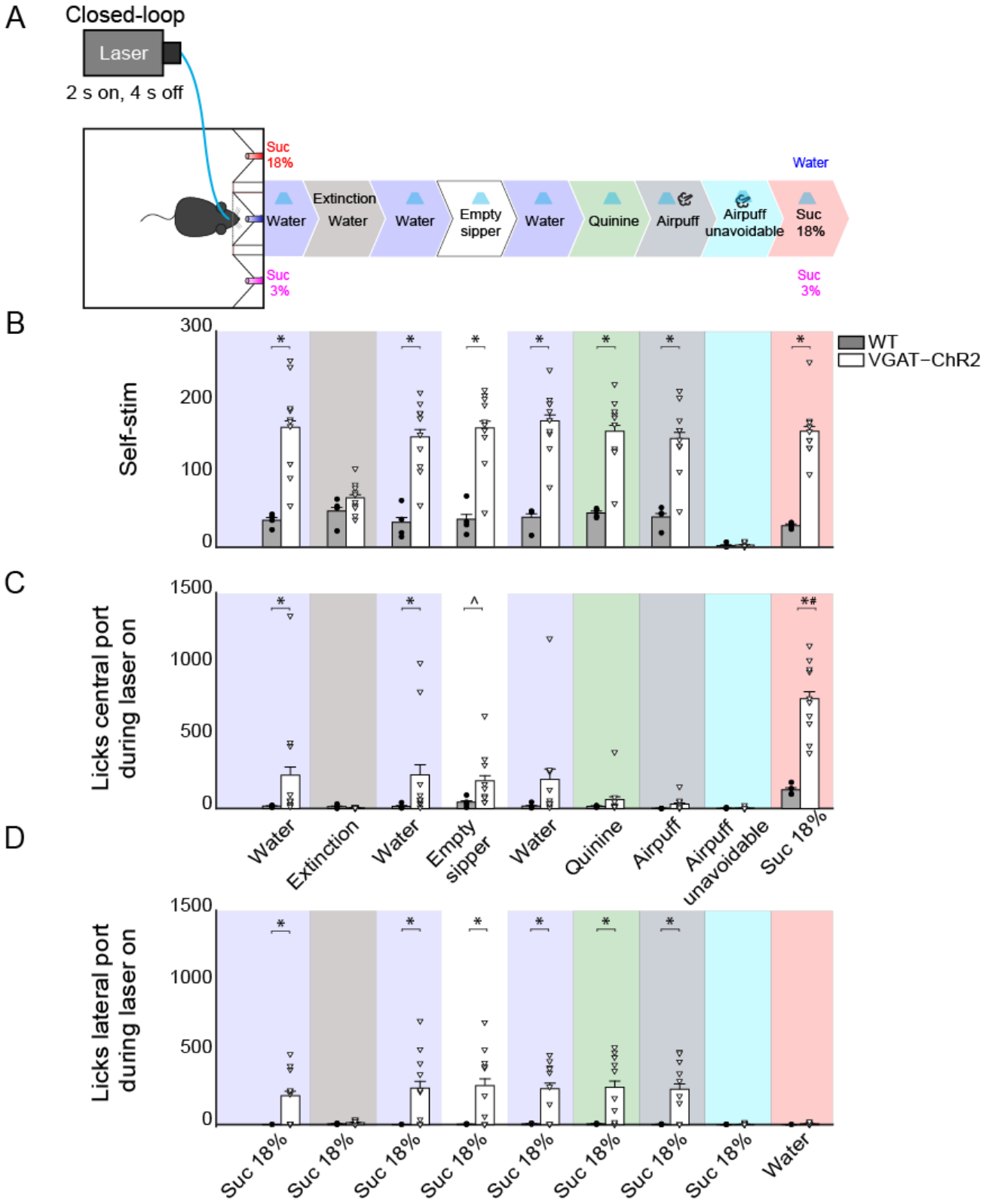

Figure 10. Activating LHA^{Vgat+} neurons does not induce the intake of a bitter tastant, nor an unavoidable aversive stimulus, but it increases the consumption of sucrose. **(A)** Schematic of behavioral setup showing stimuli delivered at central port. The water stimulus in the central port was replaced by an empty sipper, quinine, or airpuff. In all phases, head-entry in the central port triggered

the laser, except in the airpuff unavoidable condition, where the first lick delivered both the laser and the airpuff. Finally, the airpuff in the central port was replaced by sucrose 18%. **(B)** The number of opto-self-stimulations given for each stimulus. The VGAT-ChR2 mice performed more self-stimulations compared with WT, except during extinction sessions and when the airpuff was unavoidable. **(C)** The number of licks given to the central port. The licks in the central port decreased when an aversive stimulus was present, such as quinine or airpuffs. In contrast, a non-edibles stimulus such as an empty sipper elicited more licks from VGAT-ChR2 mice ($p < 0.05$). Moreover, when sucrose 18% was in the central port, VGAT-ChR2 group increased its consumption substantially compared with WT. **(D)** The number of licks in the lateral port containing sucrose 18% during opto-self-stimulation. The intake of the lateral port of sucrose 3 % is not shown because it was neglectable. Each dot and triangle represent a single individual. ^ Denotes statistically significant difference ($p < 0.0001$) from WT. Unpaired-Student t-test. * $p < 0.05$ relative to WT group. # $p < 0.05$ between sucrose 18% from other stimuli delivered at the central port. Two-way ANOVA followed by the Holm Sidak test.

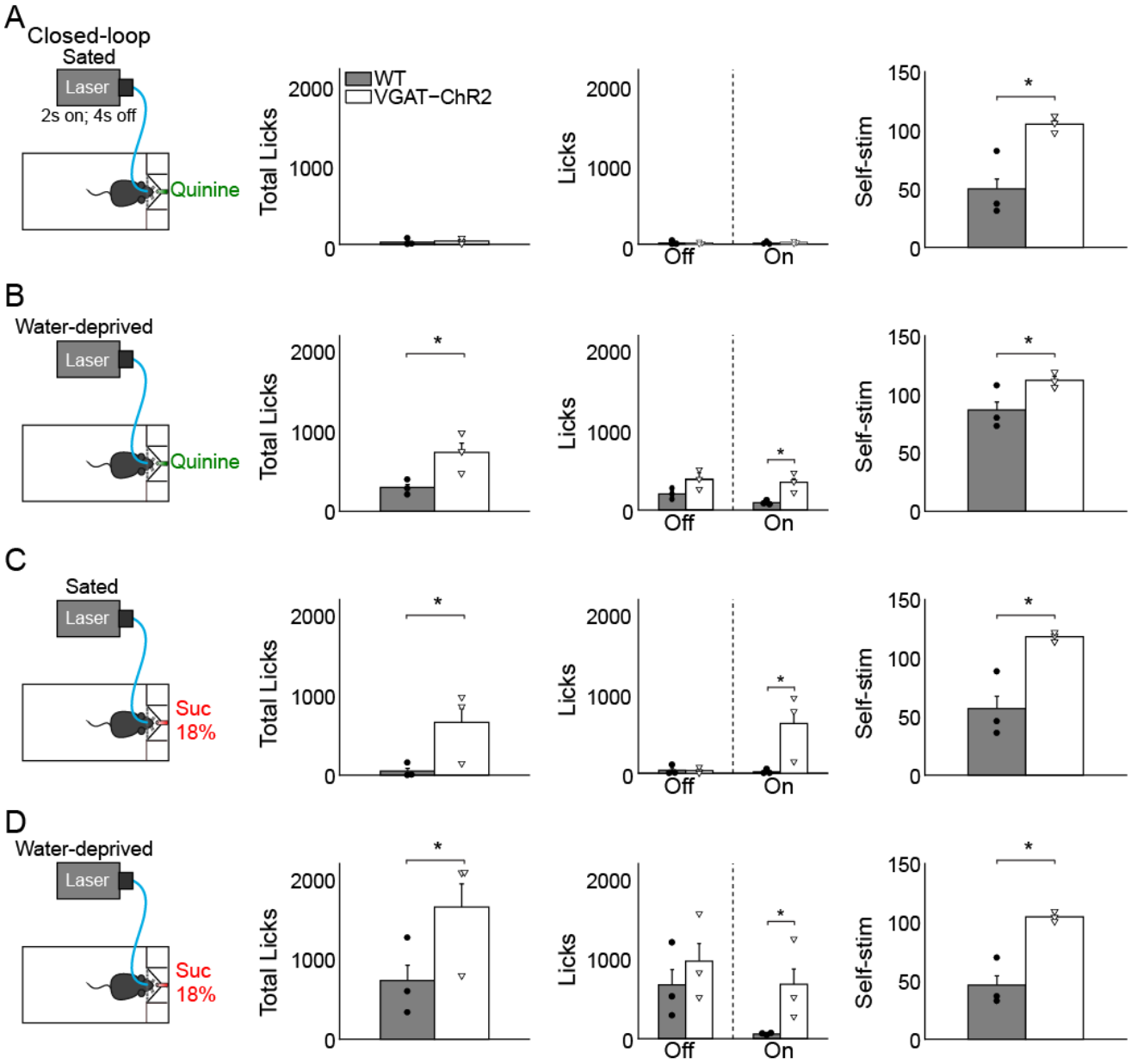

Figure 11. Water deprivation gates LHA GABAergic neurons to increase the quinine intake. **(A)** Sated mice had free access to one sipper filled with quinine. The laser was turned on in closed-loop protocol (*left panel*). In sated VGAT-ChR2 mice, activation of these neurons did not increase quinine intake (*central panels*) but continued opto-self-stimulating (*right panel*). **(B)** Water deprived transgenic mice consumed more quinine than in WT mice (*central panel*) when the laser was turned on. **(C-D)** Total licks, number of licks during photostimulation, and when the laser was turned off in the session (*central panels*). Number of opto-self-stimulations of 18% sucrose during sated and water deprivation condition (*right panel*). * $p < 0.05$ indicates significant differences compared with WT mice according to an unpaired- t-student test.

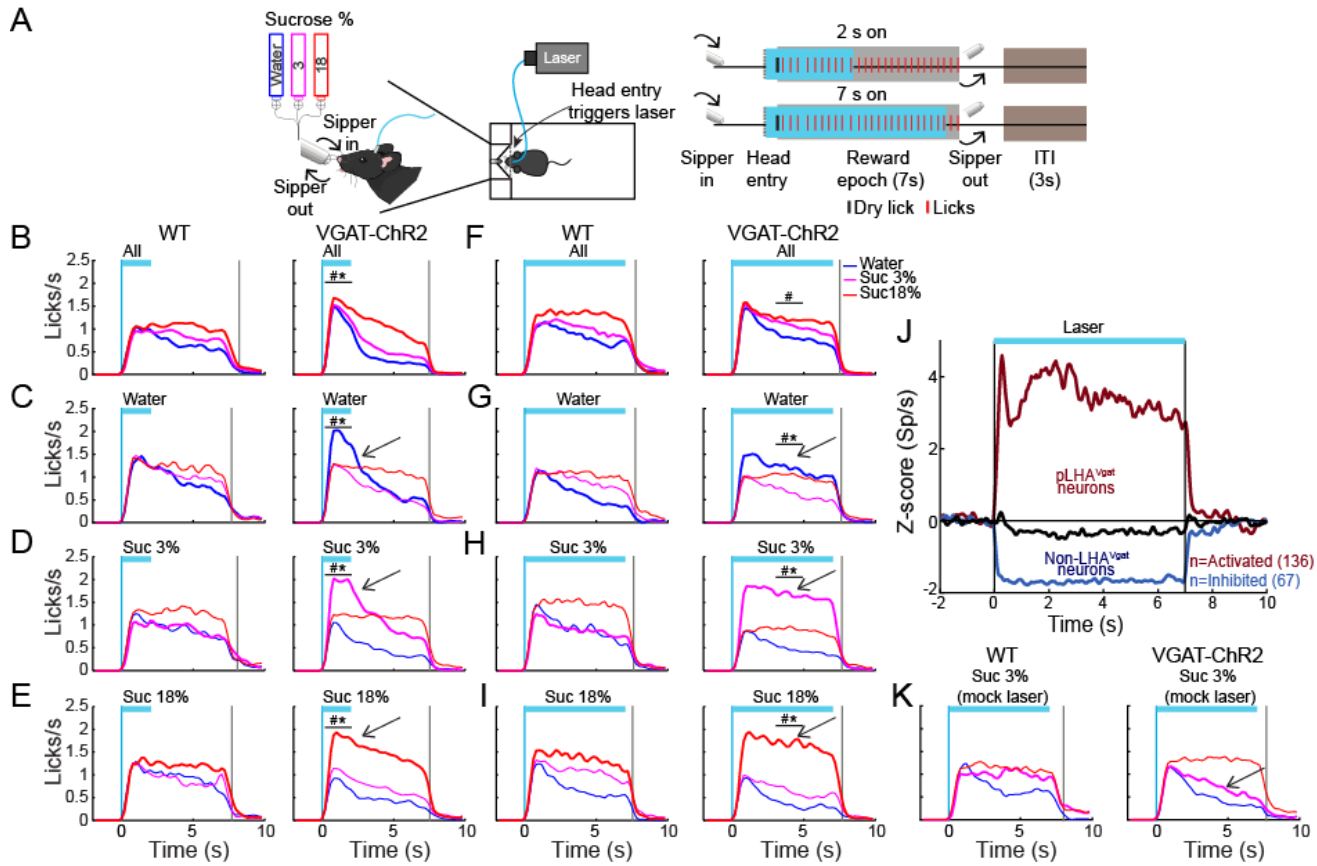

Figure 12. Activation of LHA GABA neurons enhances water and sucrose's palatability. **(A)** Closed-loop stimulation during the brief access test. *Left panel,* behavioral setup. The box contained a sipper that delivered a ~2 µL drop of either water, sucrose 3%, or 18% per lick. *Right panel*, schematics of the structure of a trial. A head entry in the port (dashed vertical line) triggered opto-self-stimulation, at 50 Hz, in some sessions for 2 s and others for 7 s (blue rectangles). The reward epoch begins with the first dry lick on the sipper (black tick) and always last 7s (gray rectangles). During the reward epoch, a drop of tastant was delivered in each lick (red marks). At the end of it, the sipper was retracted, and an Inter Trial Interval (ITS) of 3 s began. **(B-E)** Data of closed-loop for 2s stimulation in the Reward epoch. PSTH of lick rate of WT (left panel) and VGAT-ChR2 mice (*right panel*) aligned (Time = 0 s) to laser onset. Opto-self-stimulation was delivered during all trials (B) or during only water trials (C, see arrow), or sucrose 3% (D), or 18 % (E). **(F-I)** Licking responses but during 7 s opto-self-stimulation. Same conventions as in B-E. The vertical blue line indicates laser onset and gray line the end of the reward epoch. The horizontal blue line indicates opto-self-stimulation window. * Indicates significant difference ($p < 0.05$) from WT group. # $p < 0.05$ among stimuli. ***J,*** Normalized Z-score

population activity of 284 neurons recorded in LHA in VGAT-ChR2 mice (n = 3). The laser was delivered during 7 s at 50 Hz. Neuronal responses were aligned to laser onset (Time = 0 s). Red and blue colors indicate activated or inhibited laser-evoked responses, relative to baseline (-1 to 0 s). Black trace illustrates neurons unmodulated by the laser. **(K)** Mock laser stimulation did not affect palatability responses. PSTH of licking responses, opto-self-stimulation was delivered along with sucrose 3% trials during 7s (arrow). Note that both groups increased the lick rate as a function of palatability, same conventions as in B-E. To elicit mock laser stimulation, mice were connected to a mock fiber optic (with no-laser connected), whereas the real fiber was glued outside the mice's head to emit blue light.

Supplementary Material

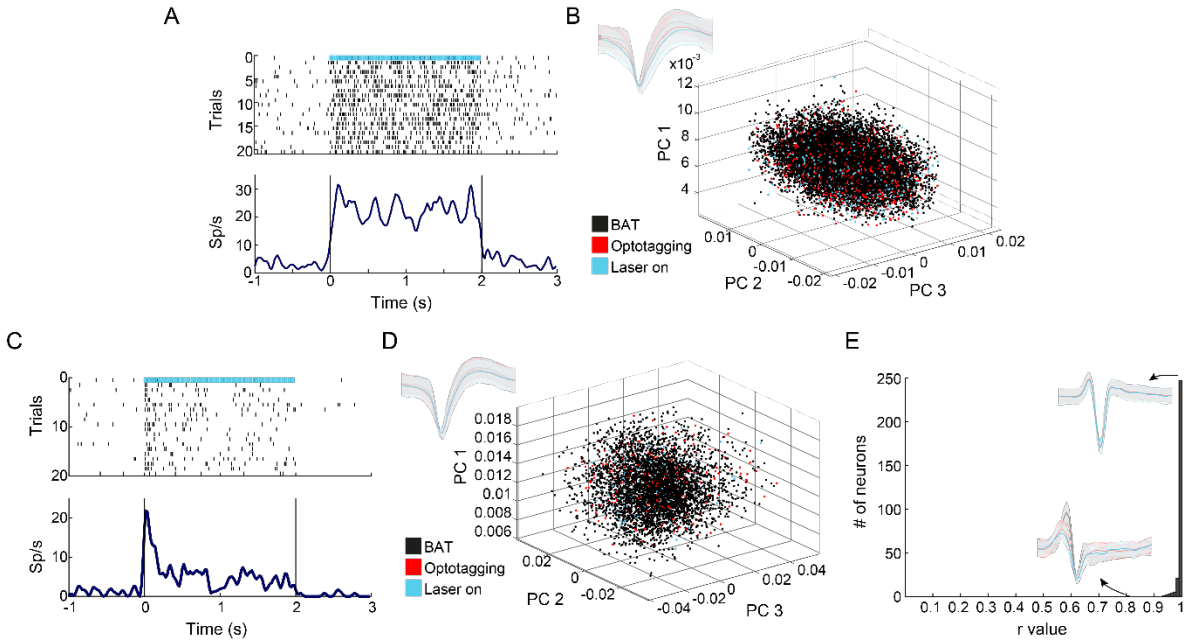

Supplementary Figure 1. Waveform stability in extracellular recordings of LHA neurons across the brief-access test (BAT) and the optotagging session. **(A)** Representative raster plot of a LHA^{Vgat+} neuron recorded during the optotagging session. Spiking responses were aligned (Time = 0 s) to the first laser pulse. Black ticks depict action potentials and blue marks on top, laser pulses (at 50 Hz). For visualization purposes, it is only shown laser pulses in the first trial. Below, PSTHs (Spikes /s, Sp/s). Vertical black lines indicate laser onset (Time = 0 s) and offset (Time = 2 s), respectively. **(B)** *Inset upper left* depicts average waveforms of a single neuron showed in A across the BAT (black), the optotagging stimulation (red), and when the laser was turned "on" (blue). Right, each dot represents an action potential during the entire session (same color-coded). Values are plotted in a three-dimensional space computed with the first three principal components (PCs) of the waveforms. **(C-D)** Same conventions as in (A-B). ***E,*** Histogram of the Pearson correlation coefficients of waveforms recorded during BAT against those recorded in the optotagging session. Waveforms depict two examples, one depicting the worst and the other the best correlation included in analysis.

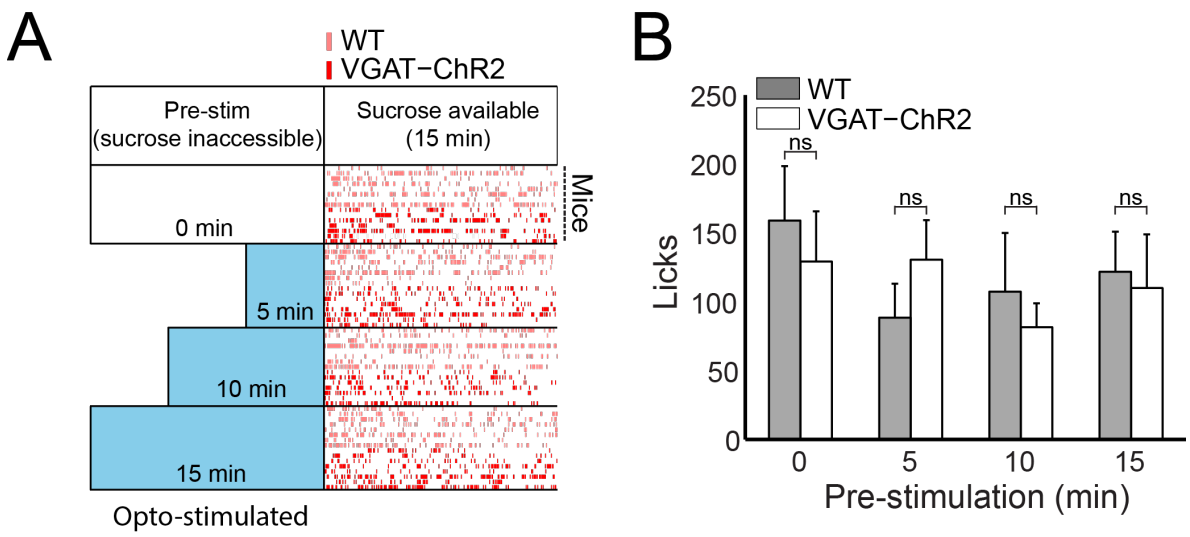

Supplementary Figure 2. Pre-stimulation of LHA^{VGAT+} neurons did not trigger a "hunger state" in that a sustained consummatory behavior is not observed. **(A)** Schematic of the pre-stimulation protocol and raster plot from VGAT-ChR2 (licks were plotted as red ticks) and WT (licks as light red ticks) mice. For this experiment, all mice underwent all pre-stimulation protocols following a Latin square design: 1) mice were pre-stimulated for either 0, 5, 10, or 15 min with no sucrose available. After pre-stimulation, mice received 15 min Free access to a sipper filled with sucrose 10%. **(B)** The average number of licks for sucrose as a function of pre-stimulation.

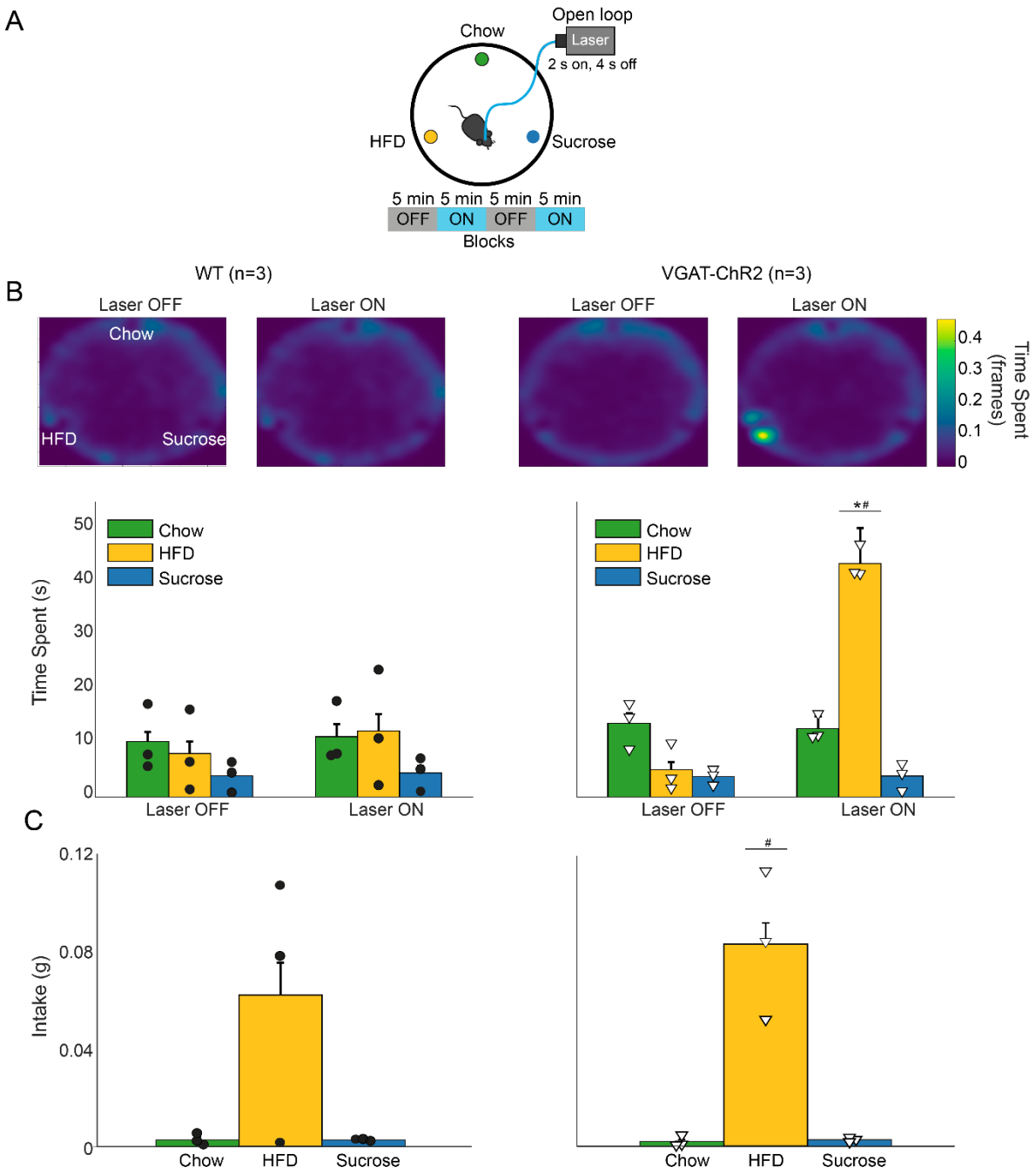

Supplementary Figure 3. Activation of LHA^{Vgat+} neurons increases the time spent near the most palatable High Fat Diet (HFD). **(A)** In a circular arena, three plates containing Chow (green), HFD (yellow), and granulated sucrose cube (blue) were available simultaneously. In a 20 min session, the laser was turned "on" following an open loop protocol (2 s on 4 s off during 5 min block with laser and 5 min with no-laser; see Figure 5A). **(B)** Average heat map and time spent in the open field. To create each heat map, we identified the centroid of the mouse at every video frame. Colorbar indicates the number of frames the subject was detected in a given pixel; higher values indicate the mice stayed in that place for a longer time. Time spent (below) was calculated as the distance between the mouse's centroid relative to each food plate. We quantify a food interaction when the subject was within 60 mm distance relative to the plate's center and remained there for at least 1 s. Each dot and triangle represent a single individual. **(C)** Intake of Chow, HFD, and granulated sucrose cube. * Denote statistically

1244 significant differences ($p < 0.0001$) relative to WT. # $p < 0.0001$ between a stimulus relative to the
1245 others. One-way ANOVA followed by the Holm Sidak test. See Video 2.

1246

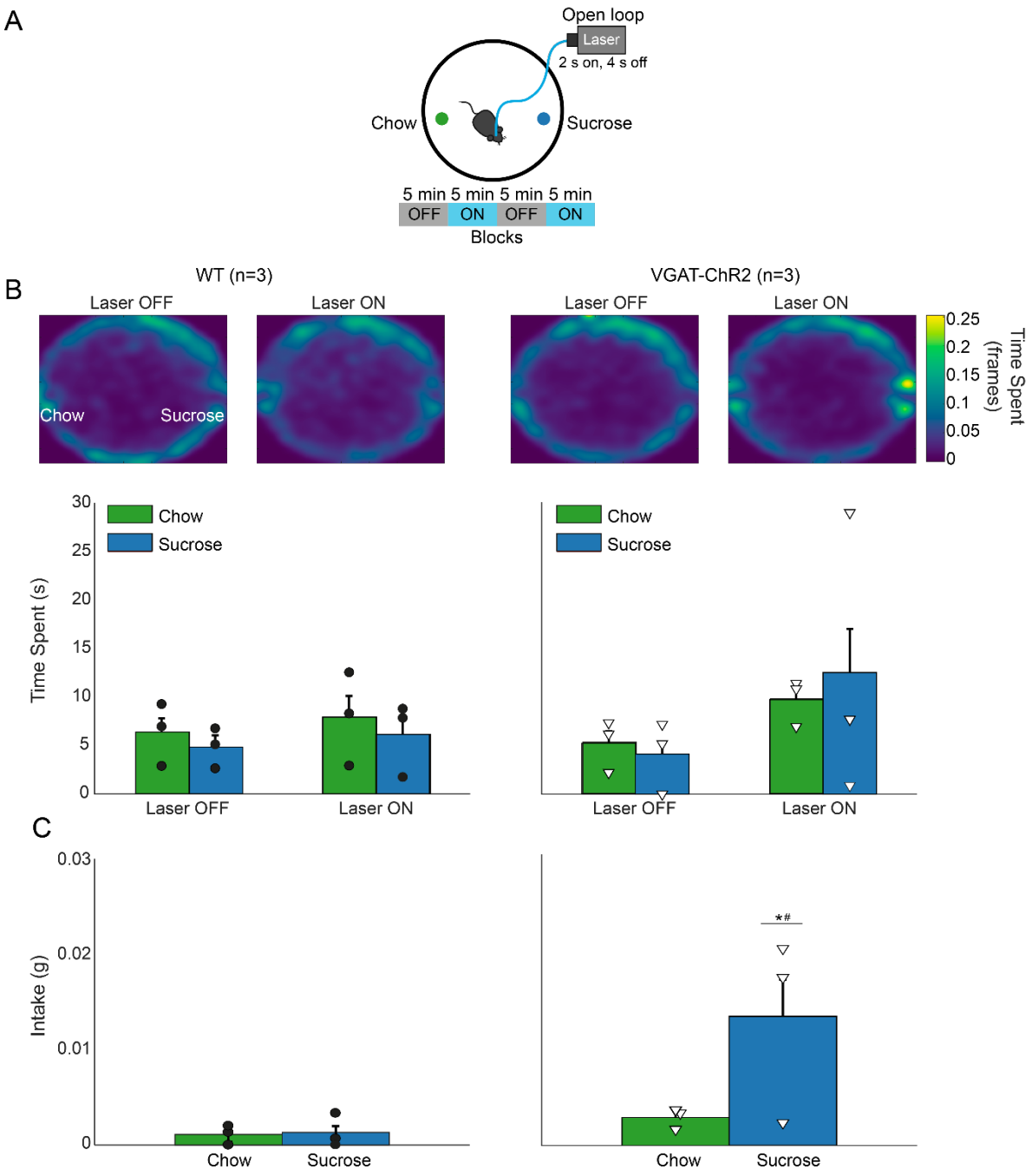

1247

1248 **Supplementary Figure 4.** Activation of LHA^{Vgat+} neurons promotes intake to the most palatable solid
1249 food. ***(A)*** In a circular arena, Chow pellet and granulated sucrose cube were presented simultaneously.
1250 The laser was turned "on" in an open loop protocol. **(B)** Mean heat map and time spent. The same
1251 conventions are in Supplementary Figure 4. **(C)** Intake of Chow and granulated sucrose cube. *

1252 Statistically significant differences ($p < 0.001$) relative to WT. # $p < 0.0001$ difference between a
1253 stimulus relative to the others. One-way ANOVA followed by the Holm Sidak test. See Video 3.

1254 **Video 1. Open loop activation of LHA^{Vgat+} neurons.** Water, 3 wt%, and 18 wt% sucrose was
1255 delivered in each port. Opto-stimulation occurred in 5 min block of no-laser and 5 min block with the
1256 laser.

1257 **Video 2. Open loop activation of LHA^{Vgat+} neurons promotes preference toward HFD over**
1258 **granulated sucrose and Chow pellet**. At equidistant position, three foods were placed on a small
1259 plate, and each contained either HFD, Chow food, or granulated sucrose cube. Opto-stimulation
1260 occurred in 5 min block of no-laser and 5 min block of the laser for 20 min.

1261 **Video 3. VGAT-ChR2 mice prefer granulated sucrose over Chow food.** Preference and intake of
1262 granulated sucrose cube vs. Chow pellet after open-loop activation of LHA GABAergic neurons.

1263 **Video 4. Closed-loop activation of LHA^{Vgat+} neurons.** Mice opto-self-stimulate in each head entry in
1264 the central licking port (where water is the nearest stimulus). Some VGAT-ChR2 mice exhibited a
1265 preference for the most palatable stimulus available (sucrose 18%), whereas others preferred the
1266 nearest but less palatable stimulus (water) over sucrose 18%

1267 **Video 5. Real-time place preference in an open field task.** At equidistant separation, four stimuli
1268 were placed on a small plate, and each contained either wood cork, Chow pellet, chocolate pellets, or
1269 a sipper a 10% sucrose solution. Mice were photostimulated by 2 s on and 4s off when crossing the
1270 designated area.

1271 **Video 6. In some VGAT-ChR2 mice, activation of LHA^{Vgat+} neurons induces gnawing to a cork**.
1272 Wood cork was placed in a transparent box, whereas mice were opto-stimulated in an open loop
1273 protocol.

1274

1275

1276

1277

1278

1279